A Bayesian Network model for bluff retreat on the southern Lake Erie coast, United States

Anthony M. Foyle[a]* and Michael A. Rutter[b]

[a] Department of Environmental Science, Penn State Erie – The Behrend College, Erie, PA 16563, USA

[b] Department of Mathematics, Penn State Erie – The Behrend College, Erie, PA 16563, USA

*Corresponding author: amf11@psu.edu; 814.898.6277

Abstract

Coastal bluffs on the 73 km Pennsylvania mainland coast of Lake Erie consist of unconsolidated glacial through paleo-lacustrine Quaternary strata overlying Devonian shale bedrock. Erosion is a significant environmental hazard on this coast where the long-term average annual retreat rate at the bluff crest is ~0.15 m/yr. As the primary geomorphic feature used to track land loss on high-relief coasts, understanding the processes that drive bluff-crest retreat and concomitant sediment and infrastructure losses remains a challenge in coastal-hazard management. This paper shows that bluff retreat on the Lake Erie coast of Pennsylvania can be successfully modeled using multivariate statistics that may have application to bluff settings across the Great Lakes basin and globally. A Bayesian Network (BN) model is developed using long-term historical data (1938-2007 training datasets) and validated against subsequent crest retreat mapped from recent lidar data. Seven field sites were sampled for environmental data that collectively covered ~30% of the 33.5 km length of the western Erie County littoral cell (WECLC). A BN with eight inputs correctly predicted bluff retreat rates for 95.4% of transects and had a mean posterior predictive probability of 84.1%. Scenarios show that greater crest-retreat rates were more likely to be associated with greater wave impact hours, less-resistant stratigraphy, narrower beaches, lower and steeper bluffs, a more energetic run-up regime, and a lower or absent bedrock-toe ledge. These diagnostic attributes should be useful across the WECLC to help identify, with finer spatial resolution, sectors with higher probabilities of having or developing significant erosion problems.

Key Words

Bluff crest retreat, Bayesian network, wave impact hours, Lake Erie

Introduction

Bedrock cliffs, unconsolidated bluffs, and low-relief banks characterize ~80% of global coasts (Emery and Kuhn, 1982). On the North American Great Lakes, just over 40% of the Lake Erie perimeter consists of bluffs and banks dominated by unconsolidated Quaternary-age sediments (Cross et al., 2016; Knuth, 2001; Pope et al., 1999; Stewart, 2001). The 73 km Pennsylvania mainland coast of Lake Erie consists of a sequence of glacial, glacio-lacustrine, and paleo-lacustrine strata overlying a discontinuous ledge of Devonian shale at the bluff toe. Regional climate trends over the next several decades (Karl et al., 2009; Lofgren et al., 2011, 2002; Shortle et al., 2015) may lead to greater bluff instability and land loss due to (i) increased erosion associated with surface runoff because of changes in precipitation duration, intensity and seasonality, and (ii) greater groundwater flux through the bluff face. Potentially mitigating this, a possible increase in regional evapotranspiration across the Great Lakes Basin may lead to lowered levels for Lake Erie, which would have a bluff-stabilizing effect as the wave regime is displaced from the bluff.

Erosion is pervasive on Great Lakes bluffs in response to Holocene lacustrine and subaerial processes, and spatial and temporal variability in retreat rates is the norm (Amin, 1989; Brown et al., 2005; Chrzastowski and Trask, 1996; Cross et al., 2016; Davidson-Arnott, 2016, 1990; Dawson and Evans, 2001; Foyle, 2018; Foyle and Schuckman, 2021; Griggs and Patsch, 2004; Griggs and Trenhaile, 1994; Hampton and Griggs, 2004; Hapke et al., 2009; Jones and Hanover, 2014; Kastrosky et al., 2011; Knuth, 2001; Luloff and Keillor, 2016; Mickelson et al., 2004; Morang et al., 2011; Ohm, 2008; Sterrett and Edil, 1982; Swenson et al., 2006; Trenhaile, 2010, 2009; Zuzek et al., 2003). Understanding bluff evolution and predicting future locations of the bluff crest, which is the standard feature used to track land loss on bluff coasts, remain challenges in coastal-hazards management (Castedo et al., 2012; Collins and Sitar, 2008; Edil and Vallejo, 1980; Hapke and Plant, 2010; Hapke and Reid, 2007; Johnsson, 2003; Mickelson et al., 2004; Moore et al., 1998; OMNR, 2001; Sunamura, 1983, 1982; Trenhaile, 2009; Witter et al., 2007; Young, 2018). The challenges exist because numerous intrinsic and extrinsic variables, including internal geotechnical properties, topography, hydrology, lacustrine and subaerial processes, and climate, act in concert to dictate the location, timing, and rates of irregular and episodic bluff retreat.

Bluff retreat is a significant environmental hazard on the entire Pennsylvania bluff coast where the long-term average crest retreat rate is ~0.15 m/yr (PA DEP, 2021). Along the western Erie County littoral cell (WECLC), the focus area for this study (Fig. 1), long-term retreat rates vary spatially and temporally but average ~0.25 m/yr by municipality along the updrift (southwest) sector, and ~0.1 m/yr along the downdrift (northeast) sector (PA DEP, 2021). Infrequent and large rotational slumps can result in 10s of meters of localized land loss over several weeks, while chronic soil creep can lead to more widespread but less significant land loss across larger tracts of bluff face. Bluff retreat along the WECLC results in a permanent loss of ~70% of the sediment volume (fines) to deep-water areas below wave base, while ~30% (sand-boulder sized material) is stored on beaches and transported downdrift in the littoral stream to one of Lake Erie's largest sand spits at Presque Isle State Park (Foyle and Schuckman, 2021).

Areas where bluff retreat creates a substantial threat to safety or structures are classified by the Pennsylvania Department of Environmental Protection (PA DEP) as Bluff Recession Hazard Areas (BRHAs) under the Bluff Recession and Setback Act (1980) (BRSA, 1980; PA DEP, 2013). Within BRHAs, new construction and certain modifications to structures are subject to a minimum bluff setback distance (MBSD) requirement. PA DEP identifies MBSDs on the basis of forward projection of the long-term bluff-crest retreat rate for a municipality and a 50, 75, or 100 yr building/infrastructure lifetime (Foyle and Rafferty, 2017). Individual municipalities have either adopted the MBSDs or have established more-stringent setbacks that range from 8-61 m (PA DEP, 2013). Because of the number of environmental variables involved, and the need for adaptive management-compatible information in erosion management decision-making, there is a benefit in moving from traditional deterministic methods towards probabilistic approaches to assessing land-loss hazards due to bluff retreat on the Great Lakes. Approaches such as BNs allow results to be expressed probabilistically, often more desirable to coastal-managers and stakeholders for decision-making purposes.

This paper examines bluff erosion on the Pennsylvania coast to determine if bluff-crest retreat can be successfully modeled using multivariate statistical methods that may have future application to similar unconsolidated bluff settings across the Great Lakes basin. A Bayesian Network (BN) approach aims to (i) improve understanding of processes and geomorphologies associated with coastal land loss on this high-relief unconsolidated coast, (ii) identify the relative roles of the principal driving forces and boundary conditions, and (iii) examine less/more energetic wave run-up regimes and low/high crest retreat-rate scenarios to identify associated or diagnostic bluff attributes. These wave-impact and retreat-rate scenarios may occur currently in the dataset at different WECLC sites due to variability in bluff morphology and in hydrodynamic and subaerial driving forces; or potentially on a future WECLC in response to climate-related environmental changes (reviewed below). The BN model is developed using real and proxy long-term historical data (1938-2007 training datasets) and validated against recent retreat rates (the BN response variable) mapped from 2007-2015 lidar data. The 2007-2015 era falls within a longer 1999-2013 era of just-below-average Lake Erie levels transitioning to a rise in lake level (2013-2020) that by mid-2019 culminated in the highest monthly-average lake levels in over a century at 175.18 m above mean sea level (175.18 m MSL; NOAA, 2022).

Field Sites

Seven ~1.5 km long field sites were sampled for environmental data that collectively cover ~30% of the 33.5 km length of WECLC coast (Fig. 1). Each site was mapped for gross bluff stratigraphy to estimate resistance to erosion; hindcast wave climate, foreshore slope and backshore elevation to estimate wave impact hours at the bluff; beach width and backshore height above lake level; bedrock height or absence at the bluff toe; bluff crest elevation; and hydrology and stratigraphy to estimate groundwater flux by watershed through the bluff face. The seven sites were selected to be representative of six HUC-12 watersheds, five coastal municipalities with BRHAs along the WECLC, and geomorphologically distinct coastal sectors. Coastal engineering structures were not considered in site selection nor included in the BN. Along the entire 33.5 km WECLC, the bluff toe is protected by ~170 short groynes, and by seawalls along just ~11% of its length. Five of the seven field sites had no seawalls or groynes (Sites 1STGL, 2RACK, 3EBSP, 4LECP, 7BMDR in Figs. 1, 2) and one had a single groyne (Site 5YMCA). One site (Site 6LSCC) had a relatively high structure density (six 8-20 m groynes; two seawalls totaling 110 m) and was downdrift of a nine-groyne field and a short-jetty pair at the mouth of Walnut Creek (Fig. 1). Consequently, the BN developed in this paper is biased towards natural bluffs where bluff slopes, beach volumes, and wave impact at the bluff are not directly influenced by the presence of engineering structures. Elsewhere, on the California coast, Hapke and Plant (2010) found that a BN had less predictive skill for more-engineered (71%; San Diego) versus less-engineered (89%; Santa Barbara) coastal regions. Gutierrez et al. (2015) incorporated proximity to anthropogenic modifications in a BN for barrier-island shoreline change in response to sea-level rise on the mid-Atlantic bight and observed some influence. However, results from the WECLC in this paper suggest that coastal-structure density is sufficiently low on the WECLC, and specifically within and near field sites (e.g., results from Site 6LSCC were not noticeably different from other sites), that it may not have significant effects on BN predictive skill.

BN Modeling

A BN is an equation-driven statistical model that uses pertinent attribute and process variables and their conditional probability dependencies to describe system behavior or an outcome of interest such as bluff-crest retreat. It uses Bayesian inference to model conditional dependencies (edges) between variables (nodes) in a directed graph or network. (Bayes, 1763; Charniak, 1991; Chen and Pollino, 2012; Gelman et al., 1995; Heckerman and Wellman, 1995; Jensen, 2001; Korb and Nicholson, 2004; Pearl, 1988; Scutari, 2010; Uusitalo, 2007). Probabilistic links between variables are illustrated by the directed graph that describes the network. BNs can both describe the relationships between variables as well as predict or explain consequences if prior conditions and behaviors are known (Charniak, 1991; Chen and Pollino, 2012; Uusitalo, 2007). Each variable is represented by one or more conditional discrete probability distributions, while connections reflect which variables relate to each other and to the BN variable of interest being modeled. Prior and conditional probabilities describe the variables and relate them to each other, and the resulting BN can be used to make probabilistic outcome predictions that can be updated as new data become available (Gutierrez et al., 2015, 2014; Mahler et al., 2012). BNs are capable of learning causal relationships between variables and can show good prediction skill even with small sample sizes. Effectively, the sample size dictates the number of classes (bins) used for each variable, with two to ten being typical (Gutierrez et al., 2011a, b; Hapke and Plant, 2010; Plant et al., 2016; Uusitalo, 2007). This study ultimately uses a 9-variable x 5-bin BN model.

When carefully designed, BNs can explain the occurrence and scale of geohazards such as bluff retreat by defining joint-probability density functions that relate forcing variables, prior behavior, and initial (boundary) conditions to geologic change. Recent geoapplications include cliff and landslide analysis (Lee et al., 2002, 2001; Lee and Choi, 2004; Mahler et al., 2012; Van Westen et al., 2003), soil quality analysis (Back, 2007), groundwater flow (Fienen et al., 2013; Li and Jafarpour, 2010), subsurface geomodeling (Gonzalez et al., 2016; Buland and Omre, 2003), and coastal hazards (Gutierrez et al., 2015, 2014, 2011a,b; Hapke and Plant, 2010; Plant et al., 2016; Sanuy et al., 2020). Hapke and Plant's (2010) application on the California coast concluded that BNs built using long-term historical data correctly forecast recent (short term) bluff retreat at over 70% of transects modeled. Similarly, high success rates were reported by Dahal et al. (2008) for landslide hazards in the Himalayas (~88% of forecasts correct) and by Gutierrez et al. (2014) who reported success rates of 68% when predicting shoreline change for a US ocean-coasts dataset. Bluff retreat on the Lake Erie coast is amenable to BN analysis because suitable training and testing geodata can be compiled for the procedure (Foyle, 2018; Foyle et al., 2021). Geodata can be developed that define pre-existing conditions (e.g., bluff slope and elevation; beach width and height; bluff toe and bedrock elevations), controlling processes (wave impact; groundwater flux), and long- and short-term crest retreat rates (1938-2007, prior behavior; 2007-2015) to train and test a BN.

Coastal Geomorphology

On Pennsylvania's 73 km mainland bluff coast, the WECLC stretches ~33.5 km from a small headland at the OH-PA state line downdrift to a large terminal groyne where Presque Isle (a Holocene flying sand spit) joins the mainland (Fig. 1). About 2 km west of the WECLC, 1.8 km-long breakwaters at Conneaut Harbor, OH, may be a more appropriate updrift littoral cell boundary than the state-line headland used here (Fig.

1). However, because this 2 km of Ohio coast was not adequately covered by lidar it is not included in this analysis. Long-term littoral sediment transport on this sand-starved, historically eroding, coast is to the northeast at 13,000-61,000 m^3/yr (Carter et al., 1987; Cross et al., 2016; Foyle and Schuckman, 2021; Knuth, 2001; Morang et al., 2011). Lakefront bluffs occur along ~88% of the WECLC coastline, the remainder comprising creek mouths and associated floodplain banks (~7%), and small ravines (~5%). Most of the bluffs directly face the open lake, with ~5% being obliquely offset from the shoreline due to floodplain reentrants at creek mouths. The lakefront bluffs reach maximum elevations of 212.3 m MSL, or 38 m above Spring 2015 lake level of 174.25 m MSL (i.e., 38 m LL). Over the past century, bluffs have supplied ~95% of the material moving in the littoral sediment stream (Cross et al., 2016; Foyle and Schuckman, 2021; Knuth, 2001). An in-depth review of coastal geomorphology and processes on this coast, and prior research by others, is provided in Foyle (2018) and Foyle et al. (2021).

The WECLC nearshore comprises shale bedrock with a patchy veneer of mud, silt, and sand within 1 km of the shoreline (<10 m water depths) that becomes more continuous offshore (LESEMP, 2021). Ten-meter and shallower bathymetric contours are approximately shore-parallel for the updrift two-thirds of the cell. Along the downdrift third, a subaqueous shoal extends ~12 km updrift from Presque Isle (near Sites 6LSCC and 7BMDR), the 10 m isobath moves to ~3.5 km offshore, and the nearshore sediment cover becomes more continuous (LESEMP, 2021). Beaches are generally narrow (<10 m) and thin (< 1 m at the backshore-bluff transition) and were present along ~70% of the WECLC during the 2018-2019 period of high lake levels. The maximum active-beach width of ~70 m occurs updrift of the large terminal groyne at the downdrift end of the WECLC, east of Site 7BMDR. On the bluffs, largely cohesive, unconsolidated, strata locally overlie as much as 3 m of shale bedrock at the bluff toe (Fig. 2). The susceptibility of the WECLC coast to erosion is enhanced because it is a northwest-facing, windward coast with a maximum wave fetch of over 200 km and dominant wave energies from the west-northwest. Landward of the bluffs, a lakeward-sloping paleo-lacustrine coastal plain with several paleo-shoreline (beach-ridge) complexes extends ~6 km inland (Schooler, 1974). The beach-ridge complexes formed during a punctuated late-Pleistocene drop in Lake Erie levels prior to Holocene lake-level rise (Coakley and Lewis, 1985; Holcombe et al., 2003). The youngest beach-ridge complex (~12,700 yrs bp; Herdendorf, 2013), which intersects the Site 4LECP bluffs, is an analog of the modern Presque Isle sand spit and sits ~30 m above modern lake level (Fig. 2).

Foyle et al. (2021) recognized that associations can be expected between physical processes, geomorphologic attributes (those used in the BN are summarized in Table 1), and bluff retreat rates on the WECLC, but that consistent and diagnostic correlations were not always evident. Figure 3 shows bluff slope, beach width, and beach thickness (variables used in the BN model) at the seven WECLC sites.

When compared with Fig. 4, which summarizes associated crest-retreat rates over different time intervals, some general correlations are apparent. For example, Foyle et al. (2021) found that Site 2RACK had the greatest long-term bluff retreat rate among sites: it had the lowest top-bedrock elevation in the entire WECLC (Fig. 2; approx. -2 m LL) and second-lowest beach width and thickness (Fig. 3), while wave impact hours (not shown here) were the second highest. Site 5YMCA had the second-lowest long-term retreat rate among all sites and this was accompanied intuitively by a moderate beach width and thickness (Fig. 3), moderate to high erosion resistance, among the lowest wave impact hours of all sites, and a low groundwater flux (not shown). In contrast, at Site 7BMDR, the long-term retreat rate was relatively constant (Fig. 4), yet the site was characterized by a general decline in bluff slope and by an increase in beach width and thickness in the downdrift direction that would intuitively be associated with reduced crest retreat. WECLC bluff behavior is thus controlled by complex interactions of multiple variables that should be amenable to BN modeling to better resolve relationships between processes, morphologies, and crest-retreat rates.

Figure 4 highlights a significant difference between long-term and short-term retreat rates on the WECLC west of Site4LECP. This may be related to construction of Conneaut Harbor (2 km updrift) between the mid-1800s and mid-1900s. Offshore sand deflection and updrift-fillet and harbor accretion likely induced a littoral sediment deficit and development of an erosional embayment (Terpstra and Chrzastowski, 1992) downdrift that extended into the WECLC that was captured in the 1938-2007 crest-retreat data. Cross et al. (2016) estimated that there was a 75% drop (to 10,300 m^3/yr) in littoral sand transport into Pennsylvania between the 1860s and 1930s, compared to pre-construction rates, and a further decline to 0 m^3/yr between the late 1930s and earliest 2000s (Foyle and Schuckman, 2021). It is possible that the deficit was partly mitigated by a resumption of some natural bypassing at Conneaut Harbor (no available data) and by intermittent anthropogenic bypassing in the 2000s (Cross et al., 2016; Hapke et al., 2009; PA DEP pers. comm., 2021). Because bedrock is below lake level along most of the western WECLC, bluff-toe erosion may be particularly sensitive to littoral-sediment supply disruptions. The return of a partial littoral sediment supply from Ohio could have led to growth of bluff-protecting beaches and an associated reduction in the recent bluff retreat rates seen in Fig. 4.

Climate Change, Lake Erie Levels, and Lakefront Bluffs

Lake Erie water level, an important driver of bluff retreat on the Pennsylvania coast (via wave attack and beach erosion/accretion), remains difficult to predict for the 21st century in the face of ongoing climate change (Angel et al., 2018; Gronewold et al., 2013). This is because of climate-model resolution and integration challenges; data limitations and uncertainty in modeling precipitation, runoff, evaporation, and lake-level responses; and complicated feedbacks between climate and earth-surface processes generally. In general, older modeling efforts tended to predict lowered future lake levels under warming climate scenarios while more-recent efforts using updated models are more likely to predict higher lake levels. Thorough reviews of Great Lakes climate, hydrology, and water-level modeling efforts are presented in Lofgren and Rouhana (2016a, b) and Kayastha et al. (2022).

Shortle et al. (2015, 2009) noted that Pennsylvania's current warming and increasing-precipitation trends are expected to continue at an accelerated rate over future decades. Similar trends were predicted for the Great Lakes basin by Notaro et al. (2015). It is feasible that warmer temperatures with increased non-frozen precipitation may lead to greater groundwater recharge of bluff surficial aquifers and increased bluff instability. Angel and Isard (1998) noted an increase in the frequency and intensity over the 20th century of cyclones traversing the Great Lakes Basin. Wang et al. (2012) documented a decline in lake ice cover over the past several decades while Desai et al. (2009) showed that lake wind speeds have been increasing. A recent review by Angel et al. (2018) concluded that Great Lakes surface temperatures have been increasing, lake ice cover declining, (down 71% between 1973 and 2010), and seasonal water-column stratification beginning earlier. Along with warmer winters that may ultimately drive snowfall events to rain with consequent impacts on lake levels and bluff stability, these trends are expected to continue in future decades. In their review, Angel et al (2018) noted that continued declines in ice cover could lead to increased damage to coastal infrastructure (and thus coastal zones) by winter storms.

Quigley et al. (1977) showed that a rise in Lake Erie level during a typical decadal scale lake-level cycle causes increased wave energy and erosion at the bluff toe. Modeling by Lofgren et al. (2002) showed that moderate warming and precipitation increases in the Great Lakes Basin could lead to higher lake levels. Cruce and Yurkovich (2011) expected coastal erosion rates to increase for Lake Erie due to more frequent storms and storm surges, and greater coastal wave energies, associated with less lake-ice cover. Basin modeling results also suggest that climate warming may result in increased precipitation in winter and spring with less frozen precipitation in future decades (Karl et al., 2009; Lofgren et al., 2011; Cruce and Yurkovich, 2011). Notaro et al. (2015) modeled late-21st century annual average lake levels to reach as much as 0.32 m above mid-20th century average levels, with peak seasonal levels occurring in mid-summer as is the case today. Using recent advanced 3D modeling, Kayastha et al. (2022) predicted that Lake Erie by mid-21st century may have average monthly levels ranging from 0.05 m below to 0.54 m above 2010-2019 levels (using individual downscaling models). Using a three-model ensemble average, Lake Erie levels may reach as much as 0.28 m above 2010-2019 levels.

Conversely, possible increases in lake evapotranspiration and a reduction in surface-water inflows to the Great Lakes basin could lead to lowered Lake Erie levels. However, the validity of some lowered-level predictions has recently been questioned (Notaro et al., 2015; Lofgren and Rouhana, 2016a, b; Xue et al., 2022) because of known limitations in older models. Modeling by Hayhoe et al. (2010) predicted that Lake Erie levels may fall over the next century to about 0.25 m below the long-term average lake level. Angel and Kunkel (2010) modeled end-21st century lake levels in response to future emissions scenarios and found large ranges in predicted levels that were sensitive to both the emission scenario and uncertainty in the models: predicted Lake Erie levels ranged from 1.0 m above to 2.0 m below 1970-1999 levels. Four different models run by Lofgren et al. (2011) predicted levels at the end of the 21st century to range from 1.45 m below to 0.33 m above long-term average. MacKay and Seglenieks (2013) predicted mid-21st century Lake Erie levels to be close to present levels. Recent modeling by Lofgren and Rouhana (2016b) suggested that Lake Erie levels had a greater than 75% probability of being lower by the late 21st century. Lake lowering should have a bluff-stabilizing effect as the impacts from hydrodynamic processes (wave attack) would be removed from the bluff (Foyle, 2018). Other changes in the system, such as a possible change in the seasonal lake level minimum-maximum range (Notaro et al., 2015) may lead to changes in wave runup at the bluff toe during typically stormy fall-to-spring seasons. Notaro et al. (2015) modeled late-21st century annual average lake levels that could decline to as much as 0.24 m below mid-20th century average levels with the peak seasonal level occurring in winter rather than during the summer months as is the case presently.

Based on the review above, there is thus a spectrum of possible future lake-level outcomes and some debate concerning the likelihood of lowered future lake levels. For the purposes of developing wave impact and bluff-crest retreat scenarios used later in this paper, we make a reasonable inference that climate warming through the 21st century could potentially lead to Lake Erie and the Pennsylvania coastal zone having the following attributes: higher lake levels; less lake and shore ice cover; a more energetic storm regime; greater bluff runoff and groundwater fluxes; more wave impact hours at the bluff; narrower beaches (due to limited accommodation space at the bluffs); less beach and bluff-face seasonal freezing; and a decrease in the effectiveness of existing coastal engineering structures. Conversely, future possible climate cooling is inferred to be associated with the opposite attributes.

Methods

BN Model Design

In this study, a BN was designed and trained on historical datasets (1938-2007) to predict bluff change that could be validated against a recent (2007-2015) observational dataset. The model assumes that future retreat of the bluff crest will occur under similar conditions to those that caused past retreat, and that historical environmental conditions along the WECLC did not change significantly between the late 20th and early 21st centuries.

The BN was built using the R statistical programing language (R Development Core Team, 2020) and the *bnlearn* package (Scutari, 2010). Geodata were compiled at individual and groups (sectors; see below) of shore-normal transects spaced at 20 m intervals along each WECLC site (Table 1). These transects were cast using the US Geological Survey's Digital Shoreline Analysis System ArcGIS extension (DSAS Version 4.0; Thieler et al., 2009). The observed field data were binned so that discrete probability distributions were generated for each input variable and the response variable. A model-fitting process based on k-fold cross validation determined which variables were related (connected nodes) and which variables were independent (unconnected nodes), although all were assumed to be connected to the observed 2007-2015 retreat rate. The output of the model was a discrete probability distribution that predicted the probability of observing different retreat rates conditional on the observed input values. The modeling approach followed here used a model-fitting process with incorporation of some expert opinion (e.g., identification of input variables) to determine which variables were related. By allowing a model-fitting process to lead in identifying the connections between variables, possible new connections applicable to this geographic region could be discovered, rather than exclusively assuming that connections that exist elsewhere must also apply here.

To prepare the data for modeling, each observed input and the 2007-2015 crest-retreat rate were discretized as categorical variables by placing each observation into one of five bins. The default binning option was to calculate the minimum and maximum for each input and create bin ranges that were of equal size spanning the range of observed values. However, in certain instances, this resulted in bins that contained zero or few observations. Because of this, bin ranges were then manually edited to ensure that observations were about equally distributed among bins while also allowing bins with larger counts to exist when many observations were observed in that range. Because there are no widely accepted automated data-discretization methods for BNs, five bins were chosen for each variable based on expert knowledge of the variables, the real-world significance of the bin breaks and, given the sample size, minimizing the number of bins with small observed counts. This is a common approach used in BN modeling of coastal systems (Hapke and Plant, 2010; Gutierrez et al., 2015, 2011). Only transects in which all input variables and a 2007-2015 retreat rate were present were used during the model fitting process, resulting in 414 transects with usable data (88% of the original 470-transect dataset).

BN Model Selection

To determine which combination of pre-identified inputs best modeled the bluff system, k-fold cross validation was used (Scutari, 2010). A value of k=10 was chosen, and the cross validation was repeated 50 times for each set of variables to ensure that there was sufficient randomization such that results would be reproducible. For each cross-validation run, the model fit with the training data was used to predict a 2007-2015 retreat rate (testing data). Comparing the predicted 2007-2015 retreat rate to the observed retreat rate measured from lidar determined the quality of each model fit. All sampling locations were equally likely to be placed into the calibration and validation groups. It was assumed that sampling locations were independent and identically distributed, and since the sampling design did not include repeated measures or a long time series of data, this assumption was appropriate. Because the k-fold cross-validation was repeated 50 times, this minimized any one cross-validation run oversampling or undersampling any one site or region.

In lieu of creating a theoretical BN before the data were collected, a model selection process was used to find the optimal BN based on the data collected. All possible 511 models using nine possible model inputs were examined. This included all nine inputs individually, all combinations with two model inputs, all combinations with three model inputs, and so forth with the last model tested using all nine inputs. A BN model was created for each combination of inputs by forcing all inputs to influence the 2007-2015 retreat rate and at the same time allowing the model fitting process to learn any additional relationships between the remaining inputs using a hill-climbing model-fitting process (Scutari, 2010). The k-fold cross validation procedure measured the percentage of correct classifications for the testing subset, averaged over the k=10 folds for each of the 50 cross-validation runs. The set of inputs with the highest percentage of correct k-fold cross validation classifications was determined to be the best-fitting model of those examined and was chosen as the final, optimal model. A classification was determined to be correct if the predicted 2007-2015 retreat rate with the highest probability matched the observed 2007-2015 retreat rate. To determine the importance of inputs in the final model, a Morris sensitivity analysis was conducted (Morris, 1991).

Geospatial Data Inputs

The inputs used in the BN are described below and summarized in Table 1. They comprise (i) a long-term (historical) bluff retreat rate (1938-2007) as a *prior-behavior* parameter; (ii) six *initial-state* parameters: bluff erosion resistance, bluff height, bluff toe elevation (or beach backshore thickness), bluff slope, top-of-bedrock elevation, and beach width; and (iii) groundwater flux through the bluff face and wave-impact hours at the bluff toe as the two expected dominant *forcing agents* across the WECLC. The model was then validated against 2007-2015 bluff-crest retreat observations mapped from 1-m digital elevation models (DEMs). Intuitively, bluffs with greater wave-impact hours, slope, elevation, and groundwater flux; and lesser beach width, toe elevation/beach thickness, top-bedrock elevation, and bluff erosion resistance should retreat faster than bluffs with the opposite characteristics: BN modeling tries to estimate likely retreat rates for the large number of combinations of these variables.

Wave Climate

Wave climate influences the severity of potential erosion on the lower bluff face that occurs due to the momentum of impacting waves, scouring by water-entrained materials, and hydraulic- and air-blasting within fractures and voids in the bluff face. Prior work by Amin (2001) on the western WECLC, and by Dawson and Evans (2001) nearby in Ohio, suggested that wave-induced erosion on Lake Erie bluffs is focused primarily on the lowermost 1.5-2 m of the bluff face (below elevations of ~176 m MSL).

Hourly wave run-up in excess of bluff-toe elevation was the hydrodynamic metric of interest, ultimately expressed as yearly wave impact hours (WIH). Because Lake Erie levels fluctuate seasonally by ~0.5 m between a summer high and a winter low, wave run-up elevations were measured relative to an average warm-season high lake level and an average cold-season low lake level baseline that varied annually (NOAA, 2022). Periods of shore and lake-ice in the WIS dataset dampen winter wave heights and reduce WIH to near-zero for one to two months during most winter seasons (Foyle et al., 2021).

To derive wave run-up elevations, hourly wave hindcast statistics modeled from the wind field were retrieved from the US Army Corps of Engineers WIS website (WIS, 2021) for three synthetic wave gauge stations equally spaced at ~8 km intervals along the WECLC in water depths of 13-16 m. Significant deepwater wave height (H_{m0}; averaged ~0.6 m), wave period, and wave direction were extracted from the WIS datasets. Waves were refracted from their hourly approach angle towards the ~N65^{0}E (sector and site dependent) shoreline orientation using equations from Komar (1998). Wave statistics for the Jan 2007- Dec 2014 time period (70,080 hrs; data were unavailable for 2015) were obtained from Station 92039 (applied to Sites 1STGL, 2RACK, and 3EBSP), Station 92036 (for Sites 4LECP and 5YMCA), and Station 92034 (for Sites 6LSCC and 7BMDR). Wave climate during the 2007-2014 time period was considered a good proxy for post-1938 historical wave climate. Because of the spatial scale of the wave-field data, wave climate was not resolved to the scale of individual transects at each site (20 m) but was instead resolved to the scale of multi-transect sectors (100-500 m) within sites: sectors were variable-length stretches of coast with uniform coastal orientation.

Wave run-up is defined as the wave set-up due to wind stress (η; mean water surface elevation relative to still lake level), plus the swash run-up (S), which is the variation in the water-beach contact elevation about the swash-backwash mean (Melby, 2012). An $R_{2\%}$ criterion, a threshold that captures the highest 2% of waves above still water level (Ruggiero et al., 2001, 1996; Stockdon et al., 2006), was used for the morphodynamically intermediate-to-reflective WECLC beaches. Specifically, the general form of the $R_{2\%}$ equation (Stockdon et al., 2006; Eqn. 1 below) was used to calculate each transect's hourly $R_{2\%}$ value from the WIS parameters and the sector-average beach foreshore slope (B_f). In Eqn. 1, the first term-group is wave set-up (η), the second term-group is swash run-up (S), Ho is significant wave height, and Lo is wavelength.

$$R_{2\%} = 1.1\left[\left[(0.35B_f\,(Ho/Lo)^{0.5}\right] + \left[\frac{(HoLo\,(0.563B_f^2 + 0.004))^{0.5}}{2}\right]\right] \qquad (1)$$

The foreshore slope (B_f) is the mean slope of the beach profile measured within 2σ above and 2σ below still lake level, where σ is the standard deviation in the offshore significant wave height (Melby, 2012). Here, B_f was measured between the shoreline and $+2\sigma$. The hourly $R_{2\%}$ values (in meters) were then compared with sector-average bluff-toe elevations to estimate cumulative wave-impact hours at the bluff for each transect within each site sector. During major autumn/winter storms, the $R_{2\%}$ value could exceed 3 m on steeper, more-windward sectors, whereas the average WECLC bluff-toe elevation was just ~1.2 m above still lake level.

An hourly $R_{2\%}$ elevation (m) in excess of the toe elevation was treated as one WIH and is distinct from the wave impact height metric of Brown et al. (2005) and Swenson et al. (2006). The WIH metric was selected in preference to the latter for the WECLC because of errors that could have arisen when trying to determine wave impact height (or cumulative wetted meters of bluff face). These errors could arise because of inconsistent slope and topographic resolution on the bottom 1-2 m of the bluff where slopes could attain ~120^0 (at topples and wave-cut notches); lidar-return clutter could occur due to patchy accumulations of dead trees at the bluff toe; and 1-20 cm thick resistant sandstone sills in the bedrock ledge would have hindered wave climb. Wave impact height would likely show greater variability by site sector than yearly WIH: the western sector at Site 2RACK and the eastern sector at Site 4LECP, for example, had 8-year total WIH counts within 3% of each other (6968 and 6785 hours, respectively) but a rough estimate of cumulative wetted bluff height differed by ~33% (4224 m vs 3184 m). The $R_{2\%}$

criterion may overestimate wave impacts at the bluff on transects where beaches are wide because a wide backshore allows more attenuation of a wave bore that may otherwise reach and climb the bluff face: incorporating a beach-width variable in the BN at least partly addressed this limitation.

WIH at the bluff face was compiled for two to six sectors at each site and varied both within and between sites due to the degree of beach development (slope, width and thickness), bathymetry, and site orientation relative to the long-term average wave-approach angle (~N61^{0}W). Sector WIH values ranged from zero to almost 39,200 hours over the eight-year data period. On average, the bluffs at the seven sites experienced ~874 wave-impact hours (~36 days) per year (Table 1).

Bluff Stratigraphy and SPR Erosion Resistance

The stratigraphy of the WECLC bluffs influences the resistance of the bluff face to the effects of gravity, wave attack, groundwater flux, and surface runoff. Stratigraphy at the WECLC sites shown in Fig. 2 is inferred to be a good proxy for the stratigraphic make-up of the bluffs since 1938. Effects due to variability in unit thicknesses and geometries of stratigraphic surfaces such as the Devonian bedrock-Quaternary till contact within the volume of bluff eroded since 1938 were inferred to be small.

Bluff stratigraphy and geotechnical information were compiled from field observations and from the literature (Amin, 2001, 1989; D'Appolonia, 1978; Buyce, 1987; Cross et al., 2016; Dawson and Evans, 2001; Highman and Shakoor, 1998; Jones and Hanover, 2014; Knuth, 2001; Knuth and Lindenberg, 1995; Terracon Consultants, Inc., 2018; Urban Engineers of Erie, Inc., 2004). Stratigraphy and standard-penetration resistance data (SPR; in blows/m, or BPM) were then expressed numerically as relative bluff resistance to erosion, which was the sum of the proportion of each of one to five stratigraphic units present at a site, times that unit's BPM value. The bluff SPR erosion resistance could not be resolved to DSAS transect scale (20 m) due to data-density limitations but was determined for each WIH site sector. From top to base of the bluffs, the BPM values for the stratigraphic units shown in Fig. 2 were estimated to be: 26 BPM for highstand paleo-strandplain sands and gravels; 35 BPM for transgressive glacio-lacustrine silts and sands; 69 BPM for medium-stiff (upper) till; 158 BPM for very stiff fractured (lower) till; and 836 BPM for Devonian shale bedrock (Foyle et al., 2021).

The presence of a shale bedrock ledge at and above the shoreline can result in large jumps in the SPR erosion resistance score because BPM values for bedrock are at least an order of magnitude greater than those for the unconsolidated strata that dominate the bluff. The least resistant paleo-strandplain sands and gravels were present only at Site 4LECP in the Trout Run watershed (Fig. 2), while resistant shale was absent (i.e., below lake level) from Sites 1STGL and 2RACK in the Turkey Creek watershed. SPR erosion resistance values ranged from 51 to 133, with a mean and median of 76 and 66, respectively (Table 1).

Long- and Short-Term Retreat Rates

Incorporating long-term retreat rates as a prior-behavior input helps train the BN to better predict outcomes such as bluff retreat, an approach that has been successful on the California coast (Hapke and Plant, 2010; Hapke and Reid, 2007). When combined with the many other variables in the BN, this prior-behavior input does not necessarily lead to bias in the model output. On the WECLC, the 1938 bluff crest was provided as a line feature for inclusion in the project GIS by the US Army Corps of Engineers, Buffalo District (W. Cross, pers. comm., 2017). The bluff crest was originally mapped from 1938 aerial photography by the US Geological Survey, did not include a crest elevation, and the horizontal uncertainty was estimated to be ±10-15 m. A spring 2007 LAS dataset, with a nominal point spacing of 1.4 m, was obtained from Pennsylvania Spatial Data Access (pasda.psu.edu). The horizontal accuracy was ±0.77 m RMSE. An inverse-distance weighted (IDW) 2007 digital elevation model (DEM) was generated from the subset of classified lidar ground points using a 1-meter (3.2 ft) cell size to facilitate direct comparison with the higher-resolution 2015 DEM generated from a spring 2015 LAS dataset using a 1-meter (3.2 ft) cell size. The 2015 DEM had a nominal point spacing of 0.7 m, was also obtained from PASDA, and had a horizontal accuracy of ±0.18 m RMSE (Foyle et al., 2021).

The 2007 and 2015 DEMs, along with derivative bluff-slope maps and hillshade surfaces were used to identify the bluff crests, which were commonly associated with a relatively sharp break in terrain slope. The break from flat or gently sloping terrain landward of the bluff face to steeper slopes (>18^0) on the bluff face was delineated as the bluff crest on both DEMs. DSAS with a 20 m shore-normal transect spacing calculated crest retreat rates (end-point rates in m/yr) for the 1938-2007 prior-behavior period and the 2007-2015 validation period at each of 470 transect-crest intercepts. Calculating rates using a linear-regression approach (Crowell et al., 1993; Honeycutt et al., 2001; Thieler et al., 2009) was not conducted because only two bluff-change eras were available. The uncertainty in the annualized rates of bluff-crest retreat for the 69-yr period is estimated to be ±0.18 m/yr, while for the 8-yr comparison it is ±0.17 m/yr (Foyle and Schuckman, 2021). The 2007-2015 annual retreat rates show occurrences of apparent bluff progradation (Fig. 4), partly a consequence of locally imprecise crest identification due to masking by bluff-edge trees. Most of the progradation data points lie within the uncertainty range for these data (±0.17 m/yr) and all were discounted to zero-change. Long-term crest retreat rates ranged from 0 to 0.9 m/yr, with a mean and median of 0.31 m/yr and 0.28 m/yr, respectively. Short-term retreat rates ranged from 0 to 1.12 m/yr, with a mean and median of 0.11 and 0.09 m/yr, respectively (Table 1).

Bluff Crest Height

Bluff crest height in meters above mean sea level (m MSL) was derived from the 2007 DEM at each DSAS transect. Published vertical accuracy for the LAS data used to build the 2007 DEM was ±18.5 cm RMSE or better in open bare-earth areas, which is equivalent to ±36 cm at the 95% confidence level. The 2007 crest height was inferred to be a good proxy for the 1938 crest height that was an initial state for the system in the BN model (1938 crest height was not available) and was also used for the 2007-2015 validation period. The 2007 elevations ranged from 174.8-212.2 m MSL (0.5-37.7 m LL), with a mean and median of 197.8 m MSL (23.5 m LL) and 200 m MSL (25.1 m LL), respectively (Table 1).

Bluff Toe Elevation (Beach Height; if present)

The bluff toe is the contact (a GIS line feature) between the steep bluff face and either the beach backshore, the lake surface, or a low-slope wave-cut shale platform. Its elevation above lake level and susceptibility to wave attack are controlled by the thickness of the beach backshore (if present) or the height of the bedrock platform where these features abut the bluff face. Toe elevation moving east across the WECLC increased by ~2 m between sites 1STGL and 7BMDR (site-average values; Fig. 3), and typically lay between 174.5 m and 177 m MSL, or 0.25-2.75 m LL.

Toe elevation was derived from the 2007 DEM at each DSAS transect and was inferred to be a good proxy for the 1938 toe that was an initial state for the system (1938 toe height was not available). It was also used as an input for the 2007-2015 validation period. It was expected that higher bluff-toe elevations would be inversely correlated with bluff-crest retreat rates, particularly if hydrodynamic processes prevail over subaerial processes (Emery and Kuhn, 1982; Lee, 2008; Ruggiero et al., 1996). The bluff toe at the WECLC sites ranged in elevation, and the beach backshore if present therefore ranged in thickness, from 0 m LL (at lake level; no beach) to 9.2 m LL (bedrock outlier), with a mean and median of 1.2 m LL and 0.9 m LL, respectively (Table 1).

Bluff-Face Groundwater Flux

Groundwater flux through the bluff face varied across each site and along the WECLC, from 10s-100s $m^3/m^2/yr$ (Foyle et al., 2021). It varied due to changes in the sizes of the ground watersheds feeding the bluff face (several per site), groundwater volumes flowing towards the bluff, and the discharge area of the bluff face associated with a sub-watershed. Low values of groundwater flux occurred near ravines where groundwater was inferred to be more easily deflected towards ravine slopes inland of the bluff face (Buckwalter et al., 1996; Cherkauer and McKereghan, 1991; Foyle, 2014). Highest values of groundwater flux occurred at Site 1STGL where inland surface drainage was poorly developed and most groundwater was inferred to drain towards the low-elevation bluffs rather than be captured by ravines and creeks (Foyle et al., 2021).

Groundwater flux is important because it can weaken the bluff and reduce cohesiveness. Collins and Sitar (2008) noted that, on the California coast, groundwater seepage reduced tensile strength. Sterrett and Edil (1982) noted that major crest retreat on parts of the Wisconsin coast were not attributable to wave attack but to groundwater effects. Foyle (2014) noted a strong correlation between bluff retreat rates and groundwater flux east of the WECLC. Groundwater flux is a more appropriate hydrologic variable for the WECLC than rainfall because everywhere on the coast gets similar precipitation, but surface-drainage development determines how much of that water exits the bluff face. Detailed estimations of groundwater flux through the WECLC bluffs were difficult due to uncertainty in the geometry of ground-watersheds in the shallow subsurface and to limited hydrogeologic data for Erie County. Because of limitations in hydrogeologic data resolution, the flux was estimated for sub-watershed sectors (not transect scale) by dividing the bluff-face area into the volume of annual precipitation inferred to infiltrate to groundwater and discharge at the bluff face.

On high beach–ridge terrain areas with no significant surface drainage, such as in the Crooked Creek and Trout Run watersheds (Fig. 2), as much as 77% of precipitation may discharge through the bluff face, given that surface runoff and base flow capture by streams are insignificant (Buckwalter et al., 1996; Foyle, 2014). Conversely, in sub-watersheds with well-developed surface drainage systems that draw groundwater towards stream axes, as little as 15% of precipitation may discharge as groundwater at the bluff face (Foyle, 2014). While annual precipitation for Erie County over the 77-yr project window increased by ~10**%** (NWS, 2021), groundwater fluxes estimated using current precipitation data were inferred to be a reasonable proxy for fluxes during the 1938-2007 period. Fluxes at the bluff face ranged from 0.1 m^3/m^2/yr to 222 m^3/m^2/yr, with a mean and median of 36.9 m/yr and 15.0 m/yr, respectively (Table 1).

Bluff Slope

Bluff slopes generally decreased moving east across the WECLC from ~35^0 to ~30^0 (Fig. 3). Variation was significant within sites and had a range of ~20^0 in the western WECLC and ~10^0 in the eastern WECLC. Steeper bluff slopes in the western WECLC were associated with greater short- and long-term bluff-crest retreat rates (Figs. 3, 4; Foyle et al., 2021). Average bluff slope was derived from the 2007 DEM at each DSAS transect and was used as a reasonable proxy for the 1938 initial state (1938 slopes were not available) and as an initial state for the validation period. The calculated slope was the average slope along a transect determined from the vertical and horizontal distances between the crest and toe of the bluff. This was a convenient geometric simplification of the sometimes-complex slope shapes seen on the WECLC. For example, groundwater discharge at Site 2RACK locally leads to a stepped bluff profile that results from relatively rapid retreat of the upper bluff's groundwater-rich lacustrine sediments. The underlying glacial tills retreat at a slower rate, resulting in a tiered bluff geometry.

The 2007 bluff slope was used in the BN model because steeper bluff slopes have been correlated with greater bluff-crest retreat rates elsewhere (Edil and Vallejo, 1980; Emery and Kuhn, 1982; Zuzek et al., 2003). In a common failure-cycle mode of retreat for tall bluffs (Brown et al., 2005; Zuzek et al., 2003), primarily wave-driven retreat cycles between steep, unstable bluff phases and less-steep, more stable phases. The 2007 bluff slopes on the WECLC ranged from 12.3^{0} to 42.2^{0}, with a mean and median of 30.3^{0} and 31.0^{0}, respectively (Table 1).

Top-of-Bedrock Elevation

Elevation of the top of shale bedrock varied across the WECLC and internal bedding typically dipped at 0-5^{0} to the south. Its elevation at the bluff toe was difficult to resolve from the 2007 DEM alone because the bedrock face is often close to vertical. Estimating the top-bedrock elevation thus also relied on interpretation of 2015 and 2017 oblique coastal aerial photography from PA DEP, and from Fall 2018 field measurements. The elevation of the top of bedrock was inferred not to have varied significantly over the 1938-2018 time window and was thus a good proxy for the top-bedrock elevation variable used in the BN model. Bedrock elevation at the bluff toe ranged from ~172.5 m MSL (-1.75 m LL at Site 2RACK) to ~177.2 m MSL (2.9 m LL; Fig. 2) at Site 7BMDR. Both mean and median top-bedrock elevations were 174.8 m MSL (Table 1).

The top-bedrock elevation was expected to influence bluff retreat because taller bedrock meant additional erosion-resistant material within the lower bluff and a greater SPR erosion resistance score (Table 1; Fig. 2). Dawson and Evans (2001) noted that in nearby Ohio, long-term bluff retreat rates declined by ~50% once the top of bedrock reached elevations greater than 1.5 m above lake level. Conversely, a taller bedrock toe may also reduce bluff-face area through which groundwater from the surficial aquifer exits, potentially leading to higher fluxes through the unconsolidated strata and accelerated bluff retreat.

Beach Width

Beach width in the WECLC averaged almost 9 m, increased from ~4 m to ~12 m moving eastward across the WECLC, and varied within each site (Fig. 3). Greatest widths were in general updrift of short groynes and particularly at the large terminal groyne at the downdrift end of the WECLC where the beach attained ~70 m in width. A wide (and high) beach moves the toe of the bluff away from hydrodynamic forces and to a higher elevation where it is less likely to be impacted by wave run-up. Lee (2008) showed that bluff-crest retreat rates on the UK coast of the North Sea were inversely proportional to the volume of beach material present. Updrift in Ohio, bluff retreat rates were found to be 67% lower when beaches were wider than 30 m and/or lake levels were lower (Dawson and Evans, 2001). Beach width measured from the 2007 DEM was judged a somewhat reasonable proxy for beach width as an initial state for the 1938-2007 time period, with the caveat that beach planforms likely changed areally and migrated significantly since 1938. It was also used as an initial-state input for the 2007-2015 validation period. The 2007 beach, where present, ranged in width from 0.2 m to 117.3 m, with a mean and median of 8.9 m and 5.8 m, respectively (Table 1).

Results

Model Selection: Minimalist BN Models

BNs were initially generated using each input individually to determine whether any single input on its own (i.e., in a minimalist, two-node, BN) had a strong bluff-retreat predictive skill. The results are shown in Table 2 and illustrate that all single-variable BNs are poor predictors of bluff retreat and that the eight-input BN described below, by comparison, is a much superior model. The bluff face slope had the best predictive skill (BFS; 42%) among the minimalist models, while the poorest skill was associated with top shale elevation (TS; 32%). Using LTRR alone as a predictor of retreat rate is at the lowermost end of the skill spectrum, at just 33% (Table 2). This is notable because estimating future beach-shoreline and bluff-crest retreat on US coasts for hazard assessments remains heavily reliant on deterministic methods where historical change alone is used to estimate future change (Boruff et al., 2005; Foyle, 2018; Honeycutt et al., 2001). The observation that minimalist BNs do not perform well on the WECLC supports the premise that designing good probabilistic, multivariate models may be the best approach to estimating future coastal erosion rates needed in hazard and risk assessments (Foyle, 2018).

Model Selection: Multiple-Input BN Model

K-fold cross validation identified an eight-input BN to be the best-fit BN of 511 possible models generated and is shown in Fig. 5. The average percentage of correctly classified transects for this BN during k-fold cross-validation was the highest among all possible models, at 39.6%. Its structure in comparison to the leading BN from each of the other multiple-input model groups is shown in Table 3 (Row 8). Similar results were obtained for the best five-input model (39.5% correctly classified; Table 3; Row 5), indicating that the five-input model performed almost as well with fewer inputs needed. The cross-validation also showed that the most complicated model, using nine inputs, resulted in over-fitting of the data and did a poorer job with predictions (36.8% correctly classified; Table 3; Row 9) when presented with testing data.

Model Fit for the Eight-Input BN

The network represented in Fig. 5 shows the observed probability distributions for all inputs in the BN. Overall model fit was assessed by comparing the predicted 2007-2015 retreat rate to the observed retreat rate for all 414 transects. The BN correctly predicted the 2007-2015 retreat-rate bin 395 times, or for 95.4% of transects. However, this included ties where the largest predicted posterior probability was tied among two bins (80 cases) or three bins (9 cases) and the observed 2007-2015 retreat rate was among those bins. In other words, a tie occurred when an observed crest-change rate was predicted by two or three of the BN-predicted change-rate bins. If the triple-tie was excluded, prediction success was 93.2%. If all ties were excluded, the model correctly predicted 73.9% of the time.

Results are plotted in Fig. 6, which shows the observed (bars) and predicted (dots) bins for the 2007-2015 retreat-rate for all participating DSAS transects at each of the seven WECLC sites. Observed-rate and predicted-rate data voids for certain transects represent locations where at least one of the eight model inputs or the 2007-2015 retreat rate was missing (12% of transects; 56 of 470 transects). The predicted value was assumed to correctly match if the observed 2007-2015 retreat rate matched the bin with the largest predicted posterior probability. Model fits by individual sites was in general very good. Observed and predicted rates matched best at Site 4LECP where there was 100% agreement. Model predictions were poorest at Site 3EBSP where there was just under 92% agreement. Site 6LSCC, the most engineered (anthropogenically modified) of all the sites, had excellent agreement with over 98% of its transect rates being predicted correctly.

As the model output is the posterior probability of the site being classified into one of five 2007-2015 retreat rate bins, some classifications have a high level of uncertainty as the posterior probability is spread across multiple bins (high uncertainty) versus being concentrated in one 2007-2015 retreat rate bin (low uncertainty). Uncertainty in the BN predictions was assessed by averaging the predicted probability of being classified in the correct observed 2007-2015 retreat rate bin for each transect. This approach considers the confidence in predicting the correct retreat rate, not just the percentage of times the correct retreat rate is correctly predicted. For the final model, the mean predicted probability was 84.1%. If the model predicted each 2007-2015 rate perfectly this result would be 100%, while if at every site each of the five bins was equally likely the result would be 20%. The predicted probabilities by transect ranged from 14.3% to 100%, with 100% indicating that the observed short-term retreat rate was the only predicted short-term retreat rate in the BN. Of the 414 transects, 287 (69.3%) predicted the observed short-term retreat bin with probability greater than 99.99%, indicating that 7 out of 10 transects had their 2007-2015 retreat rates correctly predicted with no uncertainty.

Sensitivity Analysis of the Eight-Input BN

For sensitivity analysis, the mean predicted posterior probability of 84.1% was used as a baseline to determine the importance of each input in the model. Table 4 shows the percent reduction in the mean predicted posterior probability when the BN was recalculated without each one of the eight inputs individually. The two most important inputs in the BN were long-term retreat rate and bluff face slope, causing a 14.3% and 13.8% reduction in the mean predicted posterior probability if removed, respectively. This result indicates that without long-term retreat rate or bluff face slope, the resulting BN model had significantly fewer (69.8% or 70.3%) correctly classified transects and more uncertainty among those predictions. The effects are smaller, but still significant, for the remaining BN inputs shown in Table 4 if individually removed.

Observed Input Probability Distributions in the BN Across the WECLC

The observed distributions of the driving-force, prior behavior, and boundary-condition inputs in the BN in Fig. 5 represent the probability distributions for each input for all field conditions encountered at the seven WECLC sites. The modal value and frequency of each distribution represent the most probable state for that input on the WECLC and are as follows: erosion resistance (SPR) is low at 60-70 blows/m (34%); wave impact hours (WIH) are moderate to high at 800-1000 hrs/yr (35%); long-term retreat rate (LTRR) is moderate at 0.3-0.5 m/yr (27%); beach width (BW) is narrow at 3-7 m (44%); bluff-crest height (BCH) is large at 200-205 m MSL (36%); top-shale elevation (TS) is near lake level, at 174-175 m

MSL (31%); toe elevation/beach height (TE/BH) is low at 0.5-1.0 m LL (42%); and bluff face slope (BFS) is relatively steep at 29-33^0 (42%). Short-term retreat rate (STRR; the BN response variable) is near-zero at 0.0-0.01 m/yr (22%). TS elevations of >176 m MSL (~1.75 m LL) were observed by Amin (2001) and Dawson and Evans (2001) to be associated with a 50% decline in bluff-crest retreat rates along eastern Ohio and westernmost Pennsylvania bluffs. Table 1 and the input distributions in Fig. 5 describe the background state of the coast over the past three-quarters of a century as interpreted by the BN.

Considering that uncertainty in the LTRRs was ~0.18 m/yr (Foyle and Schuckman, 2021), retreat rates less than 0.1 m/yr were inferred to reflect bluff stability (Fig. 5; little resolvable change). Given that the median LTRR was 0.28 m/yr (Table 1), retreat rate bins with ranges below and above this value were inferred to represent low (0.1 to 0.3 m/yr) and moderate (0.3-1.0 m/yr) rates, respectively. These descriptive groupings may be of more practical use to coastal managers, are highlighted in Fig. 5, and are utilized in scenario analyses below. Long-term retreat rates along the WECLC are overall skewed towards higher rates (Fig. 5): moderate retreat rates dominate the LTRR distribution (48% probability) compared to low retreat rates (37% probability) and bluff stability (little resolvable change; 15%). The bluff state with the highest probability of occurrence on this coast is thus moderate retreat. About 85% of the bluff transects across the seven study sites retreated at least 7 m during the 1938-2007 time period (>0.1 m/yr in Fig. 5), while about 48% retreated over 23 m (>0.3 m/yr). Sixty-nine years of bluff retreat have also left almost 70% of the bluff face steeper (>29^0) than what is considered a stable slope for these types of unconsolidated bluffs in the Great Lakes region (<26.5^0; Foyle et al., 2021; OH DNR, 2011; Ohm, 2008;). These steep slopes suggest an overall dominance of hydrodynamic (wave forces acting on the lower bluff) over subaerial (runoff or groundwater discharge acting on the upper, aquifer-rich, bluff) erosion processes driving bluff retreat at the seven WECLC sites (Emery and Kuhn, 1982; Foyle, 2018).

Rate uncertainty in the STRRs was ~0.17 m/yr (Foyle and Schuckman, 2021), and values for 2007-2015 retreat of less than 0.1 m/yr were conservatively inferred to represent bluff stability (little resolvable change). The 2007-2015 rates were also grouped for scenario analyses below: stability (<0.1 m/yr), low retreat rates (0.1-0.2 m/yr), and moderate retreat rates (0.2-1.2 m/yr; Fig. 5). In contrast to the LTRR distribution, retreat rates between 2007 and 2015 are slightly skewed towards lower rates (Fig. 5), with bluff stability (0.0-0.1 m/yr) having a greater probability of occurrence (42%) than any of the other retreat-rate bins in the distribution individually. In the following sections, we use scenarios to explore how bluff attributes may change with changes in two highly visible processes on the WECLC: wave impact and crest retreat.

Wave Impact Scenarios: Comparing the Trained BN to Low-WIH and High-WIH End-Member States

Future climate change in the Lake Erie basin will likely lead to changes in environmental conditions that may lead to an increase, stasis, or decrease in bluff-retreat rates. Wave climate as the driving force in this BN (Fig. 5) is inferred to remain an important driver of bluff retreat that may be enhanced or reduced by other driving forces and boundary conditions not directly incorporated in this model (such as groundwater flux; surface runoff (overland flow); vegetation density; coastal structure attributes). As wave climate changes, the WIH at the bluff can be expected to change at any given location. As reviewed above, WIH may increase with rising lake levels (a warmer, stormier lake with less seasonal ice cover) or decrease with falling lake levels (a cooler, possibly calmer, lake with increased seasonal ice cover). WIH also changes spatially on the WECLC currently.

In this section, we examine what the trained BN reveals about bluff-system inputs under scenarios of (i) low-WIH conditions where there is a 100% probability that WIH is <500 hrs/yr and (ii) high-WIH conditions where there is a 100% probability that WIH is >1000 hrs/yr (Fig. 7), where the WIH probability distributions are separately constrained to these end-member states. Examining these end-member states helps answer coastal management questions such as *how do bluff attribute distributions differ at less-energetic versus more-energetic locations compared to the prior, unconstrained BN*? In the following discussion, bluff states will utilize the stable, low retreat, and moderate retreat bin-groupings described above because this generalization (a reduction from five data bins to three descriptive groupings) may be of more practical use to coastal managers.

BN Constrained to Low-WIH Conditions

The updated BN constrained to low-WIH conditions (Fig. 7a) shows observed input distributions across all sites when the WIH<500 hrs/yr bin has a 100% probability of occurrence versus its prior 14% probability in the unconstrained BN (Fig. 5). At the subset of WECLC transect locations where these low-WIH conditions are met, the following selected observations, summarized in Table 5, can be made:

- The LTRR probability distribution changes significantly from the prior, switching from a distribution with slightly higher probabilities of faster retreat to one strongly skewed towards slower retreat (Figs. 5, 7a). The probability of the highest retreat rates (0.5-1.0 m/yr) decreases from 21% to 2%, indicating that highest LTRRs are extremely unlikely (2% probability) to occur at low-WIH sites. The probability of moderate retreat rates (0.3-1.0 m/yr; not shown in Table 5) decreases from 48% to 14%. Stability and low retreat rates (<0.3 m/yr) increase in importance, now accounting for 86% of the distribution compared to 52% in the prior. As might be expected, stable transects (<0.1 m/yr) become more prevalent with a probability of occurrence of 38% compared to 15% in the prior (Figs. 5, 7a).

- At low-WIH sites, the BW distribution changes significantly from the prior, skewing towards wider beaches: narrow beaches less than 7 m in width decrease in probability of occurrence from 62% in the prior to 28% here. All beach width bins in the dataset experience at least some wave impact with low-WIH counts being more likely when beaches are wider. For example, low WIH counts at the bluff are more likely (57% probability) to occur where beaches are wider than 10 m.
- The TS distribution skews slightly towards overall-lower elevations, with only a 14% probability of TS being greater than the critical 176 m elevation compared to 20% in the prior. Bedrock-free transects are exceptionally unlikely (0.2% probability) to occur in association with low-WIH conditions.
- The TE/BH distribution skews towards higher values, increasing from a 28% to a 52% probability of the toe elevation or beach height being >1.5 m above lake level. This suggests that taller beaches, which afford greater bluff protection, are more likely than not to occur where low-WIH conditions prevail.
- Steep bluff-face slopes (BFS $>29^0$) have a slightly lower probability of occurrence under low WIH conditions: steep slopes formerly represented 69% of the prior distribution but now account for 57%. This suggests wave impact hours drive steeper slopes on the WECLC.
- The STRR distribution does not change significantly from the prior: this supports the premise that WIH is but one input among many that influences bluff retreat rates on this coast.

BN Constrained to High-WIH Conditions

The updated BN constrained to high-WIH conditions (Fig. 7b) shows the distributions of BN inputs across all sites when the WIH>1000 hrs/yr bin has a 100% probability of occurrence versus its prior 16% probability in the unconstrained BN (Fig. 5). At the subset of WECLC transects where these high-WIH conditions are met, the following selected observations, also summarized in Table 5, can be made:

- The LTRR distribution becomes bimodal and the probability of highest LTRR (>0.5 m/yr) almost doubles from 21% to 36%, while the probability of moderate retreat remains about the same (almost 50%; Figs. 5, 7B). The probability of stability and low retreat rates (<0.3 m/yr) also changes slightly, from 52% to 56%. Stable transects double their probability of occurrence from 15% in the prior to 30% at high-WIH locations. This counterintuitive increase may be attributable to higher top-shale elevations co-occurring at some high-WIH transects.
- The BW distribution at high-WIH sites is skewed towards narrower beaches: beaches less than 7 m in width increase slightly in probability of occurrence from 62% to 72% (Figs. 5, 7b). Widest beach-

es (>20 m) are exceptionally unlikely (0.2% probability) to be associated with high-WIH transects, suggesting a pronounced bluff-protection role played by beaches wider than 20 m on this coast.

- Taller bluffs (BCH greater than the median BCH of 200 m MSL) are only slightly more likely to occur (55% vs 49%) at high-WIH locations, where beaches also tend to be narrower than in the prior (Fig. 7b).
- The probability of TS being greater than 176 m triples from ~20% in the prior to ~61% (Fig. 7b). Field observations indicate that tall-TS areas typically have narrow beaches and function like reflective seawalls during storms.
- Steep bluff-face slopes (BFS >29^0) have a slightly higher probability (76%) of occurring at transects with high WIH counts compared to the prior (69%). This confirms a positive correlation between wave impacts, toe erosion, and bluff steepening.
- The STRR (BN response variable) distribution does not change significantly from the prior. Moderate retreat rates (0.2-1.2 m/yr; Fig. 5) that represent 38% of the distribution in the prior decrease slightly, to 31%, under high-WIH conditions:

In summary, Table 5 and Figs. 5 and 7 show that lower-WIH transects on the WECLC, compared to the prior unconstrained BN, have higher probabilities of being associated with wider beaches, lower retreat rates, greater beach volumes (both width and thickness), a lower shale ledge, and a less-steep (i.e., more stable) bluff face. The opposite conditions generally occur at high-WIH transects.

Comparing Low-WIH to High-WIH End-Member Scenarios

Knowing how low-WIH and high-WIH scenarios compare to prior "average" bluff conditions on the WECLC, we can now ask the management-related question "*how do bluff characteristics differ between less-energetic and more-energetic WECLC areas?*" Comparing the two constrained BNs (WIH<500 hrs/yr and WIH>1000 hrs/yr; Figs. 7a, 7b) can help coastal managers visualize (i) bluff processes and morphologies at more sheltered versus less sheltered locations along the present WECLC, and (ii) how attributes may change with a possible future transition to more-energetic conditions (e.g., as a consequence of higher lake levels during a warmer climate) across the WECLC. The trained BN built on three-quarters of a century of change shows that, when transitioning from low-WIH to high-WIH conditions, the following changes, summarized in Table 6, are notable:

- The SPR distribution, characterized by more-resistant bluffs (84% >70 blows/m) where low-WIH conditions prevail, skews towards less-resistant bluffs under high-WIH conditions (61% >70 blows/m).

- The LTRR distribution moves towards faster retreat rates – the probability of occurrence of moderate retreat rates (>0.3 m/yr) triples from 14% to 44% and there is a lower probability of encountering stable conditions (a 38% probability of transects showing <0.1 m/yr declines to 30%; Figs. 7a, 7b).
- The BW distribution moves towards narrower beaches, with the probability of encountering beaches <7 m wide increasing from 28% to 72%. At the widest beaches, the probability of bluffs experiencing wave impact declines from 28% to near-zero.
- BCH switches from a 26% probability of bluffs at any transect being taller than the WECLC median of 200 m, to a bimodal distribution with a 55% probability of bluffs being taller than the median.
- TS elevations are about four times more likely to exceed the critical 176 m MSL mark in areas with high-WIH conditions, the probability increasing from 14% to 61%. Narrow thin beaches are common at these wave-reflective, taller-bedrock, locations.
- The TE/BH distribution flips to a dominance by thinner beach backshores and/or lower-elevation bluff toes as WIH increases (<1.5 m; 48%->75%). This suggests a loss of beach volume and associated bluff protection under more energetic wave conditions.
- The BFS distribution moves towards the steeper-slope end of the distribution under high-WIH conditions (76% probability of being steeper than 29^0). This again points to the dominant role of hydrodynamic processes in driving bluff retreat compared to subaerial processes on this coast.
- The STRR distribution skews insignificantly towards lower rates.

In summary, Fig. 7 and Table 6 indicate that present high-WIH transects, or WECLC transects generally under future conditions where higher WIHs may prevail, have higher probabilities of being associated with no or narrower beaches, faster crest retreat, smaller beach volumes (both width and height), and steeper bluffs than their low-WIH counterparts.

Crest Retreat Scenarios: Comparing Lowest-LTRR (Stable) to Highest-LTRR (Highly Erosional) States

In this section, we examine what the BN reveals about how system inputs differ between (i) lowest-LTRR (i.e., stable) conditions where there is a 100% probability that LTRR is <0.1 m/yr (**Fig. 8a**) and (ii) highest-LTRR conditions where there is a 100% probability that LTRR is >0.5 m/yr (Fig. 8b). We can ask the management-related question *how do bluff-system characteristics differ between locations where the least erosional and most erosional conditions occur?* Answering this question can permit coastal managers to better understand why rapid retreat may occur in one area and not in another in terms of changes in the probability distributions of the other BN variables (Fig. 8). These end-member states can help in understanding bluff attributes at relatively stable versus highly-erosional locations along the present

WECLC, or across the WECLC generally under a possible transition to more-erosional conditions (e.g., during a future warmer climate with higher lake levels). When transitioning from areas experiencing stable conditions to those experiencing rapid erosion, the following changes can be observed and are summarized in Table 7:

- The SPR distribution at lowest-LTRR locations (Fig. 8a) shows that the bluffs are likely to be more erosion-resistant than at highest-LTRR sites where bluffs plot exclusively in the two lowest-SPR bins (Fig. 8b). In other words, crest stability is more likely at more resistant bluffs (Fig. 8a), while the fastest-eroding bluffs tend to be the least resistant bluffs (Fig. 8b).
- The WIH distribution skews towards a greater number of impact hours and indicates that a more intense wave regime is, intuitively, more likely to occur at higher-LTRR locations.
- The BW distribution skews strongly towards narrower beaches where LTRRs are highest: the probability of beaches being <7 m wide more than triples. Widest beaches (>20 m) are exceptionally unlikely (0.1% probability) of being associated with highest LTRRs, demonstrating the erosion-protection benefit of wider beaches.
- The BCH distribution skews towards lower bluffs under highest-LTRR conditions. Counterintuitively, taller bluffs are more likely to be associated with crest stability (Fig. 8a) while lower bluffs are more likely to be associated with greatest instability (Fig. 8b). This may be related to a probable century-scale time lag between wave-steepening at the bluff toe and subsequent crest retreat on tall Great Lakes bluffs (Brown et al., 2005).
- The TS distribution skews towards lower bedrock elevations under highest-LTRR conditions. Highest-LTRRs are most likely (71% probability) to be associated with bedrock elevation at or below lake level: they are virtually certain (>99% probability) of occurring where bedrock elevations are below the critical 176 m MSL elevation (Fig. 8b).
- The TE/BH distribution skews strongly towards lower values under highest-LTRR conditions. Highest LTRRs are virtually certain (99% probability) to occur when beaches are thin (<1.5 m; Fig. 8b) or the bluff toe lies near lake level. Stability is more likely to occur when the beach backshore is thicker than 1.5 m (63% probability) compared to when it's thin or absent (Fig. 8a). Thickest beaches are extremely unlikely (2% probability) to be associated with highest-LTRR sites (Fig. 8b).
- The BFS distribution skews towards steeper slopes under highest-LTRR conditions (Fig. 8b). Steepest bluff-face slopes are extremely unlikely (>37^{0}; 3% probability) to be associated with stable bluffs (Fig. 8a), while gentlest slopes are very unlikely (<25^{0}; 5% probability) to be associated with highly erosional bluffs (Fig. 8b). This again suggests the importance of hydrodynamic forces over subaerial forces as a primary driver of bluff retreat on this coast. If groundwater flux through upper-bluff aq-

uifers was a significant forcing agent, higher LTRRs would have a stronger association with lower BFS values.

- The STRR distribution skews towards slightly lower rates under highest-LTRR conditions. This hints that an historical period of rapid crest retreat can be followed by (or contain) a recent (or short term) period of relative stability where cyclical bluff retreat operates.

In summary, Fig. 8 and Table 7 show that higher-LTRR conditions along parts of the present WECLC, or across the WECLC generally in the future if there is a transition to higher lake levels accompanying climate change, are more likely to be associated with less-resistant bluffs, absent or narrow beaches, smaller beach volumes (narrower width and less thick), lower bluffs, a lower shale bedrock ledge, and steeper bluff-face slopes.

Discussion

The BN performs well despite the complexity of bluff-retreat processes on this coast. Current understanding of cyclical retreat at tall bluffs under wave-driven conditions in particular is that periods of enhanced toe retreat lead to steeper, less stable bluffs that then fail, causing significant crest retreat over a subsequent shorter time period. This then leads to a period of relative bluff stability and slower retreat rates until the bluff once again approaches an over-steepened future state (Brown et al., 2005; Collins and Sitar, 2008; Hapke and Plant, 2010; Mickelson et al., 2004; Zuzek et al., 2003). Work on the Lake Michigan coast shows that it may take just months to years for the bluff crest to respond to toe erosion on low (<10 m relief) bluffs but may take decades to a century on tall bluffs (>30 m; Brown et al., 2005; Mickelson et al., 2004). This cyclical behavior may be detectable in Table 7 where the highest-LTRR scenario is associated with slightly lower STRRs and the lowest LTRR scenario is associated with slightly higher STRRs: the LTRR sampling period may be capturing more than one failure cycle, while the STRR likely is not.

The BN suggests (Fig. 7; Tables 5, 6) that locations with high-WIH conditions currently (i.e., in the dataset), and potentially WECLC bluffs in general under future climate-warming where higher WIHs could prevail, have greater probabilities of being associated with no or narrower beaches, faster crest retreat, smaller beach volumes (width and height), and steeper bluffs. Similarly, higher-LTRR conditions along parts of the WECLC currently, or across the WECLC in the future if higher lake levels accompany climate change, are more likely to be associated with less erosion-resistant bluffs, no or narrower beaches, smaller beach volumes (narrower width and less thick), lower bluffs, more-energetic run-up conditions, a lower shale bedrock ledge, and steeper bluff-face slopes (Fig. 8; Table 7). These diagnostic attributes may be useful across the entire WECLC to coastal managers as supplementary data to help identify, with finer spatial resolution, bluff sites with higher probabilities of having or developing significant erosion problems. Increased probabilities of steeper bluff slopes (BFS) under both high-WIH & high-LTRR states suggest that hydrodynamic processes dominate over subaerial processes on this coast. The associations between bluff attributes and observable low/high wave energy and stable/highly erosional bluff conditions should provide useful information for hazard management and help in future coastal risk/resilience assessments on the Pennsylvania coast.

Results show that the BN has an 84.1% *mean posterior predictive probability* and a >73.9% *correct-classification rate* for all WECLC transects as a collective group: Fig. 6 shows that the model works slightly better at some sites than at others. Poor performance is not notable at any individual site, for example at the most anthropogenically modified Site 6LSCC. The BN performs well in its prediction of bluff retreat rates across the WECLC, even though the duration of the validation window is a relatively short eight years compared to the model inputs that integrate processes across an order-of-magnitude longer time window of almost seventy years. Given that bluffs normally show spatial and temporal variability in retreat rates, the BN sheds light on the approximate recurrence interval (RI) of major slump-failure events on the WECLC coast. The BN results imply that RIs are likely longer than lidar, aerial photography, and T-sheet data coverages that extend back over 140 years to the late 1870s. If catastrophic, long RI, bluff failures are rare in the post-1870s record then most retreat during the 1938-2015 observation period may be attributed to smaller, shorter-RI failures: both the 1938-2007 and 2007-2015 crest-change comparisons would then be less likely to capture catastrophic-failure events. If the RIs of large events were significantly shorter than 140 years, then a larger number of such events would likely have been captured in the 1938-2007 data than in the 2007-2015 data, and the BN predictive skill may then have degraded.

The BN developed here identifies the relative importance of eight system variables collectively to bluff retreat on the WECLC coast (Table 3). The sensitivity analysis summarized in Table 4 indicates that LTRR is an important input variable in this BN for the WECLC. To some extent, this validates the historical practice nationally of using LTRRs to estimate future land-loss hazards on coastlines when more comprehensive environmental datasets are unavailable. A possible reason for its importance is that LTRR is an integrated result of interactions among all processes and attributes contributing to bluff retreat over an extended time period. Conversely, groundwater flux appears to have a relatively minor, hard to quantify, influence on bluff behavior on the WECLC, as shown by the degradation in BN predictive skill when it is included during k-fold cross-validation (Table 3, Row 9). This is somewhat unexpected because groundwater is known to increase the number and size of slope failures elsewhere (e.g., Castedo et al., 2013; Cherkauer and McKereghan, 1991; Collins and Sitar, 2008; Sterrett and Edil, 1982). However, bluff-face slope is influenced by groundwater levels (Edil and Vallejo, 1980; Mickelson et al., 2004), so the BN may be indirectly accounting for a groundwater role through the BFS input. Anecdotally, groundwater escape at the bluff face was observed to positively correlate with enhanced bluff instability and slope reduction on the eastern Erie County coast during recent high-precipitation years. The reason for its apparent unimportance on the WECLC may also be partly due to an imperfect quantification of the groundwater flux beneath WECLC watersheds.

Conclusions

This paper shows that bluff retreat on the northwest Pennsylvania coast of Lake Erie can be effectively modeled using a Bayesian statistical approach. The BN developed for the WECLC performs well in relating processes and geomorphologic attributes along largely natural-state bluffs. At seven field sites that collectively sample 30% of the WECLC's 33.5 km extent, the BN has an 84.1% *mean posterior predictive probability* and a >73.9% *correct-classification rate* for all transects as a collective group. The BN is not degraded due to a relatively large number of anthropogenic modifications at one site in particular, Site 6LSCC. Basic two-node BNs do not perform well in this study. This supports the premise that multivariate probabilistic models are a best-practice approach to estimating future coastal erosion rates needed in future hazard and risk assessments. Because the BN works well for a diverse range of seven geomorphically representative sites, it should be adaptable to bluffs on the remainder of the Pennsylvania coast and potentially applied elsewhere on Lake Erie.

The BN suggests that locations with high-WIH conditions in the dataset currently, and potentially WECLC locations in general under future climate-warming with a more energetic wave climate, have greater probabilities of being associated with absent to narrow beaches, faster crest retreat, smaller beach volumes, and steeper bluffs. Similarly, highly erosional locations along parts of the WECLC in the dataset, or across WECLC locations in the future if higher lake levels accompany climate change, are more likely to be associated with less-resistant bluffs, absent to narrow beaches, smaller beach volumes, a lower or absent shale bedrock ledge, more-energetic run-up conditions, and lower and steeper bluffs. These attributes can be used across the entire WECLC by coastal managers to supplement existing efforts to better (with higher resolution) identify sites where moderate to high erosion rates are more likely to occur. Almost all bluff transects in the WECLC dataset experience wave impact, but fewer wave impact counts at the bluff occur where beaches are wider than 10 m, and high-WIH counts approach zero at beaches wider than 20 m. The loss of beach volume and associated bluff protection under more energetic conditions confirms an expected positive correlation between beach width and bluff erosion-protection. Increased probabilities of steeper bluff slopes under both high-WIH & high-LTRR states shows that hydrodynamic processes dominate over subaerial processes across the WECLC. This suggests that future hazard-mitigation strategies should be focused on the lower bluff and beach to reduce crest retreat in many cases.

The associations identified in the BN between bluff attributes and processes, and the likely associations between attributes and constrained low/high wave energy and stable/highly erosional conditions should prove useful for ongoing bluff erosion hazard management and future risk assessments on the Pennsylvania coast. The BN provides a probabilistic understanding of the processes and attributes associated with bluff retreat and contributes to a growing research field focused on using probabilistic methods to better quantify coastal change nationally. Because bluff retreat is controlled by many factors with spatial and temporal variation and internal feedbacks, using BNs to help identify erosion hazards and geomorphic associations is statistically stronger than relying on the traditional deterministic approach of using historical retreat rates alone in hazard assessment. The BN developed here incorporates uncertainty by recognizing the probabilistic distributions associated with driving processes, bluff attributes, and crest retreat rates. Related future research opportunities on this coast could include using BNs to help identify specific bluff reaches that respond similarly to given combinations of environmental inputs. Using BNs to provide data input for predicting future bluff-crest positions by geomorphic reach rather than by municipal jurisdictions, would likewise be a logical next step towards meeting the data needs of ongoing bluff management.

Acknowledgements

This work was supported by a research grant from Pennsylvania Sea Grant College Program through the NOAA National Sea Grant College Program. Acknowledgements are due to W. Cross at the US Army Corps of Engineers, Buffalo District, for sharing 1938 bluff-crest positional data with this project; and to K. Schuckman, Pennsylvania State University, for compiling lidar-derived bluff geospatial parameters used in the BN model. This paper benefited greatly from improvements suggested by two anonymous reviewers.

References

Amin S.M., 1989. Bluff toe erosion of Lake Erie shoreline near West Springfield, Pennsylvania. Pennsylvania Geogr. 27, 13-27.

Amin, S.M.N., 2001. Bluff response in glacial till: south shore of Lake Erie. Great Lakes Geogr. 8, 78-86.

Angel, J.R., Isard, S.A., 1998. The frequency and intensity of Great Lake cyclones. J. Clim. 11, 61-71.

Angel, J.R., Kunkel, K.E., 2010. The response of Great Lakes water levels to future climate scenarios with an emphasis on Lake Michigan-Huron. J. Great Lakes Res. 36, 51-58.

Angel, J., Swanston, C., Boustead, B.M., Conlon, K.C., Hall, K.R., Jorns, J.L., Kunkel, K.E., Lemos, M.C., Lofgren, B., Ontl, T.A., Posey, J., Stone, K., Takle, G., Todey, D., 2018. Midwest. In: Impacts, Risks, and Adaptation in the United States. Fourth National Climate Assessment, Vol. II. US Global Change Research Program, Washington, DC, pp. 872-940.

Back, P.-E., 2007. A model for estimating the value of sampling programs and the optimal number of samples for contaminated soil. Environ. Geol. 52, 573-585.

Bayes, T., 1763. An essay towards solving a problem in the doctrine of chances. Philosophical Transactions of the Royal Society of London. Reprinted by Barnard, G.A. (1958), in Biometrika 45, 293-315.

Boruff, B.J., Emrich, C., Cutter, S.L., 2005. Erosion hazard vulnerability of US coastal counties. J. Coast. Res. 21, 932-942.

Brown, E.A., Wu, C.H., Mickelson, D.M., Edil, T.B., 2005. Factors controlling rates of bluff recession at two sites on Lake Michigan. J. Great Lakes Res. 31, 306-321.

BRSA, 1980. Bluff Recession and Setback Act. Pennsylvania Code, Title 25 Environmental Protection, Chapter 85 Bluff Recession and Setback. https://www.pacodeandbulletin.gov/secure/pacode/data/025/chapter85/025_0085.pdf; Accessed July 2022.

Buckwalter T.F., Schreffler T.L., Gleichsner, R.E., 1996. Geohydrology and water quality of the unconsolidated deposits in Erie County, Pennsylvania. US Geological Survey Water-Resources Investigations Report 95-4165, Denver, CO.

Buland, A., Omre, H., 2003. Bayesian linearized AVO inversion. Geophysics 68, 185-198.

Carter, C.H., Neal, W.J., Haras, W.S., Pilkey, O.H. Jr., 1987. Living with the Lake Erie Shore. Duke University Press, Durham, NC.

Castedo, R., Murphy, W., Lawrence, J., Paredes, C., 2012. A new process-response coastal recession model of soft rock cliffs. Geomorpol. 177–178, 128-143.

Charniak, E., 1991. Bayesian networks without tears. AI Magazine 12, 50–63.

Chen, S.H., Pollino, C.A., 2012. Good practice in Bayesian network modeling. Environmental Modeling & Software 37, 134-145.

Cherkauer, S., McKereghan, F., 1991. Ground-water discharge to lakes: focusing in embayments. Ground Water 29, 72-80.

Chrzastowski, M. J., Trask, C.B., 1996. Nearshore Geology and Geologic Processes along the Illinois Shore of Lake Michigan from Waukegan Harbor to Wilmette Harbor, Contribution to the U.S. Army Corps of Engineers Illinois Shoreline Erosion Interim IV Study, Final Report. US Army Corps of Engineers, Chicago, IL.

Coakley, J.P., Lewis, C.F.M., 1985. Postglacial lake levels in the Erie Basin. In Karrow, P.F. and Calkin, P.E. (Eds.), Quaternary Evolution of the Great Lakes. Geological Association of Canada, Special Paper 30, 195-212.

Collins, B.D., Sitar, N., 2008. Processes of coastal bluff erosion in weakly lithified sands, Pacifica, California, USA. Geomorphol. 97, 483-501.

Cross, W., Morang, A., Frey, A., Mohr, M.C., Chader, S., Forgette, C.M., 2016. Historical sediment budget (1860s to present) for the United States shoreline of Lake Erie. US Army Corps of Engineers, Engineer Research and Development Center ERDC/CHL TR-16-15.

Crowell, M., Leatherman, S.P., Buckley, M.K., 1993. Shoreline change rate analysis: Long term versus short term data. Shore & Beach 61, 13-20.

Cruce, T., Yurkovich, E., 2011. Adapting to climate change: A planning guide for state coastal managers–a Great Lakes supplement. NOAA Office of Ocean and Coastal Resource Management, Silver Spring, MD.

Dahal, R.K., Hasegawa, S., Nonomura, A., Yamanaka, M., Dhakal, S., Paudyal, P., 2008. Predictive modeling of rainfall-induced landslide hazard in the Lesser Himalaya of Nepal based on weights-of-evidence. Geomorphol. 102, 496–510.

Davidson-Arnott, R., 2016. Erosion of cohesive bluffs: A discussion paper on processes controlling erosion and recession of cohesive shorelines with particular reference to the Ausable Bayfield Conservation Authority (ABCA) shoreline north of Grant Bend. University of Guelph, Guelph, Ontario, Canada.

Davidson-Arnott, R.G.D., 1990. The effects of water level fluctuations on coastal erosion in the Great Lakes. Ontario Geogr. 10, 12-25.

Dawson, S.A., Evans, J.E., 2001. Geological causes of local variation in coastal bluff recession rates, northeast Ohio shoreline of Lake Erie. Environ. Geosci. 8, 1-10.

Desai, A.R., Austin, J.A., Bennington, V., McKinley, G.A., 2009. Stronger winds over a large lake in response to weakening air-to-lake temperature gradient. Nat. Geosci. 2, 855-858.

Edil, T.B., Vallejo, L.E., 1980. Mechanics of coastal landslides and the influence of slope parameters. Eng. Geol. 16, 83-96.

Emery, K.O., Kuhn, G.G., 1982. Sea cliffs: their processes, profiles and classifications. Geol. Soc. Am. Bull. 93, 644–654.

Fienen, M.N., Masterson, J.P., Plant, N.G., Gutierrez, B.T., Thieler, E.R., 2013. Bridging groundwater models and decision support with a Bayesian network. Water Resour. Res. 49, 6459–6473.

Foyle, A.M., 2014. Groundwater flux as a determinant of coastal-zone upland loss: a case study from the Pennsylvania coast of Lake Erie, USA. Environ. Earth Sci. 71, 4565-4578.

Foyle, A.M., 2018. The Lake Erie Bluff Coast of Pennsylvania: State of Knowledge Report on Coastal Change Patterns, Processes, and Management. Pennsylvania State University. www.pawalter.psu.edu; (accessed December 2022).

Foyle, A.M., Rafferty, S.D., 2017. Bluff erosion hazards and construction setbacks on the Great Lakes coasts of the United States. Trans. Built Environ. 173, 149-160.

Foyle, A.M., Schuckman K., 2021. Reduced sediment export to the Pennsylvania Lake Erie littoral zone during an era of average lake levels. J. Great Lakes Res. 47, 1644-1655.

Foyle, A.M., Rutter, M.A., Schuckman, K., 2021. Evaluating Bluff Retreat and Sediment Supply on the Lake Erie Coast of Pennsylvania using Bayesian Network Modeling and Change-Detection Analysis. Pennsylvania State University. www.pawalter.psu.edu; (accessed June 2022).

Gelman, A., Carlin, J.B., Stern, H.S., Rubin, D.B., 1995. Bayesian data analysis, Texts in Statistical Science, Chapman & Hall, New York, NY, USA.

Gonzalez, E.F., Gesbert, S., Hofmann, R., 2016. Adding geologic prior knowledge to Bayesian lithofluid facies estimation from seismic data. Interpretation 4, SL1-SL8.

Griggs, G.B., Trenhaile, A.S., 1994. Coastal cliffs and platforms. In: Carter, R.W.G. and Woodroffe, C.D. (Eds), Coastal Evolution: Late Quaternary Shoreline Morphodynamics. Cambridge University Press, Cambridge, UK, 425-450.

Griggs, G.B., Patsch, K.B., 2004. California's coastal cliffs and bluffs. In: Hampton, M.A. and Griggs, G.B. (Eds), Formation, Evolution and Stability of Coastal Cliffs-Status and Trends. US Geological Survey Professional Paper 1693, 53-64.

Gronewold, A.D., Fortin, V., Lofgren, B., Clites, A., Stow, C.A., Quinn, F., 2013. Coasts, water levels, and climate change: A Great Lakes perspective. Clim. Change 120, 697-711.

Gutierrez, B.T., Plant, N.G., Thieler, E.R., 2011a. A Bayesian Network to Predict Vulnerability to Sea-Level Rise: Data Report. US Geological Survey Data Series 2011-601, Reston, VA.

Gutierrez, B.T., Plant, N.G., Thieler, E.R., 2011b. A Bayesian network to predict coastal vulnerability to sea level rise. J. Geophys. Res. 116, FO2009, 15 pp.

Gutierrez, B.T., Plant, N.G., Thieler, E.R., Turecek, A., 2015. Using a Bayesian network to predict barrier island geomorphologic characteristics. J. Geophys. Res. Earth Surf. 120, 2452-2475.

Gutierrez, B.T., Plant, N.G., Pendleton, E.A., Thieler, E.R., 2014. Using a Bayesian Network to Predict Shoreline-Change Vulnerability to Sea-Level Rise for the Coasts of the United States. US Geological Survey Open-File Report 2014-1083, Reston, VA.

Hampton, M.A., Griggs, G.B., 2004, Formation, Evolution, and Stability of Coastal Cliffs–Status and Trends. US Geological Survey Professional Paper 1693, Denver, CO.

Hapke, C., Plant, N., 2010. Predicting coastal cliff erosion using a Bayesian probabilistic model. Mar. Geol. 278, 140–149.

Hapke, C.J., Reid, D., 2007. The National assessment of shoreline change: Part 4, historical coastal cliff retreat along the California coast. US Geological Survey Open-File Report 2007-1133, Reston, VA.

Hapke, C.J., Malone, S., Kratzmann, M., 2009. National assessment of historical shoreline change: a pilot study of historical coastal bluff retreat in the Great Lakes, Erie, Pennsylvania. US Geological Survey Open-File Report 2009-1042, Reston, VA.

Hastie, T., Tibshirani, R., Friedman, J., 2001. The Elements of Statistical Learning. Springer Series in Statistics, Springer New York Inc., New York, NY, USA.

Heckerman, D., Wellman, M.P., 1995. Bayesian networks. Communications of the ACM 38, 27-30.

Herdendorf, C.E., 2013. Research overview: Holocene development of Lake Erie. Ohio J. Sci. 112: 24-36.

Highman, T.A., Shakoor, A., 1998. Role of soil joints in causing bluff erosion along the Lake Erie shoreline, northeast Ohio. Environ. Eng. Geosci. 4, 195-207.

Holcombe, T.L., Taylor, L.A., Reid, D.F., Warren, J.S., Vincent, P.A., Herdendorf, C.E., 2003. Revised Lake Erie postglacial lake level history based on new detailed bathymetry. J. Great Lakes Res. 29, 681-704.

Honeycutt, M.G., Crowell, M., Douglas, B.C., 2001. Shoreline-position forecasting: impact of storms, rate-calculation methodologies, and temporal scales. J. Coast. Res. 17, 721-730.

Jensen, F.V., 2001. Bayesian networks and decision graphs. Springer-Verlag, New York, NY, USA.

Johnsson, M., 2003. Establishing development setbacks from coastal bluffs. State of California, California Coastal Commission Memorandum W11.5, San Francisco, CA.

Jones, D.M., Hanover, R.H., 2014. A technique for estimating the volume of sand eroded from Lake Erie bluffs between Cleveland and the Ohio-Pennsylvania border. OH DNR, Division of Geologic Survey, Geologic Note 9.

Hayhoe, K., VanDorn, J., Croley II, T., Schlegal, N, Wuebbles, D. 2010. Regional climate change projections for Chicago and the US Great Lakes. J. Great Lakes Res. 36, 7-21.

Karl, T. R., Melillo, J. T., Peterson, T. C., 2009. Global Climate Change Impacts in the United States, Cambridge University Press, Cambridge, UK.

Kastrosky, K., Galetka, S., Mickelson, D., David, L., 2011. Developing a legally defensible setback ordinance for Bayfield County, Wisconsin. Bayfield County, WI.

Kayastha, M.B., Ye, X., Huang, C., Xue, P., 2022. Future rise of the Great Lakes water levels under climate change. Journal of Hydrology, 612(B) doi.org/10.1016/j.hydrol.2022.128205.

Knuth, P.D., 2001. Determination of sediment loading potential to Pennsylvania Lake Erie coastal waters. REP-PDK Associates and Edinboro University of Pennsylvania.

Knuth, P.D., Lindenberg, R., 1995. Monitoring bluff erosion along Pennsylvania's portion of the Lake Erie shoreline. Report to the Pennsylvania Department of Environmental Protection, Harrisburg, PA.

Komar, P.D., 1998. Beach Processes and Sedimentation, 2nd Edition. Prentice Hall, NJ, USA.

Korb, K., Nicholson, A., 2004. Bayesian Artificial Intelligence. Chapman and Hall, CRC Press, Boca Raton, FL, USA.

Lee, E.M., 2008. Coastal cliff behaviour: Observations on the relationship between beach levels and recession rates. Geomorphol. 101, 558-571.

Lee, E.M., Hall, J.W., Meadowcroft, I.C., 2001. Coastal cliff recession: the use of probabilistic prediction methods. Geomorphol. 40, 253–269.

Lee, S., Choi, J., 2004. Landslide susceptibility mapping using GIS and the weights-of-evidence model. International J. Geographical Information Sci. 18, 789–81.

Lee, S., Choi, J., Min, K., 2002. Landslide susceptibility analysis and verification using the Bayesian probability model. Environ. Geol. 43, 120–131.

LESEMP, 2021. OH DNR Office of Coastal Management, Lake Erie Shore Erosion Management Plan; (accessed June 2022). https://gis.ohiodnr.gov/MapViewer/?config=lesemp

Li, L., Jafarpour, B., 2010. A sparse Bayesian framework for conditioning uncertain geologic models to nonlinear flow measurements. Adv. Water Res. 33, 1024-1042.

Lofgren, B.M., Rouhana, J., 2016a. Physically plausible methods for projecting changes in Great Lakes water levels under climate change scenarios. J. Hydrometeo. 17, 2209-2223.

Lofgren, B.M., Rouhana, J., 2016b. Reaffirmation of large biases in a long-used method for predicting changes in Great Lakes water levels in climate change scenarios. NOAA Technical Memorandum GLERL-167, Ann Arbor, MI.

Lofgren, B.M., Hunter, T.S., Wilbarger, J., 2011. Effects of using air temperature as a proxy for potential evapotranspiration in climate change scenarios of Great Lakes Basin hydrology. J. Great Lakes Res. 37, 744-752.

Lofgren, B.M., Quinn, F.H., Clites, A.H., Assel, R.A., Eberhardt, A.J., Luukkonen, C.L., 2002. Evaluation of potential impacts on Great Lakes water resources based on climate scenarios of two GCMs. J. Great Lakes Res. 28, 537-554.

Luloff, A.R., Keillor, P., 2016. Managing coastal hazard risks on Wisconsin's dynamic Great Lakes shoreline. Wisconsin Coastal Management Program.

MacKay, M., Seglenieks, F., 2013. On the simulation of Laurentian Great Lakes water levels under projections of global climate change. Climatic Change, 117, 55-67.

Mahler, C.F., Varanda, E., de Oliveira, L.C.D., 2012. Analytical model of landslide risk using GIS. Open J. Geol. 2, 182-188.

Melby, J.A., 2012. Wave runup prediction for flood hazard assessment. ERDC Coastal and Hydraulics Laboratory Report ERDC/CHL TR-12-24. US Army Corps of Engineers, Washington, DC.

Mickelson, D.M., Edil, T.B., Guy, D.E., 2004. Erosion of coastal bluffs in the Great Lakes. In: Hampton, M.A. and Griggs, G.B. (Eds), Formation, evolution, and stability of coastal cliffs–Status and trends. US Geological Survey Professional Paper 1693, Denver, CO, 107-123.

Moore, R.J., Clark, A.R., Lee, E.M., 1998. Coastal cliff behaviour and management: Blackgang, Isle of Wight. Geol. Soc. London. Eng. Geol. Spec. Publ. 15, 49-59.

Morang, A., Mohr, M.C., Forgette, C.M., 2011. Longshore sediment movement and supply along the US Shoreline of Lake Erie. J. Coast. Res. 27, 619-635.

Morris, M.D., 1991. Factorial sampling plans for preliminary computational experiments. Technometrics 33, 161-174.

NOAA, 2022. NOAA GLERL Great Lakes Dashboard; (accessed November 2022). https://www.glerl.noaa.gov/data/dashboard/GLD_HTML5.html.

Notaro, M., Bennington, V., Lofgren, B., 2015. Dynamical downscaling-based projections of Great Lakes water levels. J. Clim. 28, 9721-9745.

NWS, 2021. NOAA National Weather Service Forecast Office. Monthly summarized precipitation data (1873-2020) for Erie, PA, from NOWData NOAA Online Weather Data; (accessed June 2021). https://w2.weather.gov/climate/xmacis.php?wfo=cle

OH DNR, 2011. Ohio Coastal Design Manual: Guidance for Professionals Designing Structures Along Lake Erie (1st Ed.). Ohio Department of Natural Resources, Office of Coastal Management, Sandusky, OH; (accessed January 2023). https://ohiodnr.gov/static/documents/coastal/ocm-guidelines-CoastalDesignManual.pdf.

Ohm, B.W. 2008. Protecting Coastal Investments – Examples of Regulations for Wisconsin's Coastal Communities. University of Wisconsin Sea Grant and University of Wisconsin-Extension, Madison, Wisconsin 38 pp.

OMNR, 2001. Understanding Natural Hazards: Great Lakes – St. Lawrence River System and Large Inland Lakes, River and Stream Systems and Hazardous Sites. Ontario Ministry of Natural Resources, Ontario, Canada, 44 pp.

PA DEP, 2013. Municipal reference document: Guidance for the implementation of the Chapter 85 bluff recession and setback regulations. Pennsylvania Department of Environmental Protection, Harrisburg, PA.

PA DEP, 2021. Section 309 Assessment and Strategy of Pennsylvania's Coastal Resources Management Program. Prepared by PA DEP Compacts and Commissions Office, Coastal Resources Management Program. June 2021, Harrisburg, PA.

Pearl, J., 1988. Probabilistic Reasoning in Intelligent Systems: Networks of Plausible Inference (2nd Ed.). Morgan Kaufmann Publishers, Inc., San Francisco, CA, USA.

Plant, N.G., Thieler, E.R., Passeri, D.L., 2016. Coupling centennial-scale shoreline change to sea-level rise and coastal morphology in the Gulf of Mexico using a Bayesian network. Earth's Future 4, 143–158.

Pope, J., Stewart, C.J., Dolan, R., Peatross, J., Thompson, C.L., 1999. The Great Lakes: Shoreline type, erosion, and accretion. 1:2,000,000-scale map sheet, US Geological Survey, Reston, VA.

Quigley, R.M., Gelinas, P.J., Bou, W.T., Packer, R.W., 1977. Cyclic erosion-instability relationships: Lake Erie north shore bluffs. Canadian Geotech. J. 14, 301-323.

R Development Core Team, 2017. R: A language and environment for statistical computing. R Foundation for Statistical Computing, Vienna, Austria; (accessed June 2022). https://www.r-project.org.

Ruggiero, P., Komar, P.D., McDougal, W.G., Beach, R.A., 1996. Extreme water levels, wave runup and coastal erosion. Proceedings of the 25th International Conference on Coastal Engineering. ASCE, 2793–2805.

Ruggiero, P., Komar, P.D., McDougal, W.G., Marra, J.J., Beach, R.A., 2001. Wave runup, extreme water levels, and the erosion of properties backing beaches. J. Coast. Res. 17, 401–419.

Schooler, E., 1974. Pleistocene beach ridges of northwestern Pennsylvania. General Geology Report 64, Pennsylvania Geological Survey, Harrisburg, PA.

Scutari, M., 2010. Learning Bayesian Networks with the bnlearn R package. Journal of Statistical Software 35, 1-22.

Shortle, J., Abler, D., Blumsack, S., and others, 2009. Pennsylvania Climate Impact Assessment. Environment and Natural Resources Institute, The Pennsylvania State University. Report to Pennsylvania Department of Environmental Protection.

Shortle, J., Abler, D., Blumsack, S., and others, 2015. Pennsylvania Climate Impacts Assessment Update. Environment and Natural Resources Institute, The Pennsylvania State University. Report to Pennsylvania Department of Environmental Protection.

Sterrett, R.J., Edil, T.B., 1982. Ground-water flow systems and stability of a slope. Ground Water, 20, 5–11.

Stewart, C.J., 2001. Open coast reach delineation and re-attribution of shore classification mapping, Pennsylvania and New York shorelines, Lake Erie – Lower Great Lakes Erosion Study. Consulting Report prepared for US Army Corps of Engineers, Buffalo, NY.

Stockdon, H.F., Holman, R.A., Howd, P.A., Sallenger, A.H., 2006. Empirical parameterization of setup, swash, and run-up. Coast. Eng. 53, 573–588.

Sunamura, T., 1982. A predictive model for wave-induced cliff erosion, with application to Pacific Coasts of Japan. J. Geol. 90, 167–178.

Sunamura, T., 1983. Processes of sea cliff and platform erosion. In: Komar, P.D. (Ed), Handbook of Coastal Processes and Erosion. CRC Press, Boca Raton, Florida, 233-265.

Swenson, M.J., Wu, C.H., Edil, T.B., Mickelson, D.M., 2006. Bluff recession rates and wave impact along the Wisconsin coast of Lake Superior. J. Great Lakes Res. 32, 512–530.

Terpstra, P.D., Chrzastowski, M.J., 1992. Geometric trends in the evolution of a small log-spiral embayment on the Illinois shore of Lake Michigan. J. Coast. Res. 8, 603-617.

Thieler, E.R., Himmelstoss, E.A., Zichichi, J.L., Ergul, A., 2009. Digital Shoreline Analysis System (DSAS) version 4.0: An ArcGIS extension for calculating shoreline change. US Geological Survey Open-File Report 2008-1278, Denver, CO.

Trenhaile, A.S. 2009. Modeling the erosion of cohesive clay coasts. Coast. Eng. 56, 59-72.

Trenhaile, A.S. 2010. Modeling cohesive clay coast evolution and response to climate change. Marine Geology 227, 11–20.

Uusitalo, L., 2007. Advantages and challenges of Bayesian networks in environmental modelling. Ecol. Model. 203, 312–318.

Van Westen, C.J., Rengers, N., Soeters, R., 2003. Use of geomorphological information in indirect landslide susceptibility assessment. Nat. Hazards 30, 399-419.

Wang, J., Bai, X., Hu, H., Clites, A., Colton, M., Lofgren, B., 2012. Temporal and spatial variability of Great Lakes ice cover. J. Clim. 25, 1318-1329.

WIS, 2021. US Army Corps of Engineers, Wave Information Studies; (accessed June 2021). www.wis.usace. army.mil

Witter, R.C., Allan, J.C., Priest, G.R., 2007. Evaluation of coastal erosion hazard zones along dune and bluff-backed shorelines, southern Lincoln County, Oregon: Seal Rock to Cape Perpetua. Open-File Report O-07-03, State of Oregon Department of Geology and Mineral Industries. Portland, Oregon.

Xue, P., Kayastha, M.B., Ye, X., Huang, C., 2022. Future rise of the Great Lakes water levels under climate change. Abstracts, AGU Frontiers in Hydrology Meeting 2022, San Juan, Puerto Rico.

Young, A.P., 2018. Decadal-scale coastal cliff retreat in southern and central California. Geomorphol. 300, 164-175.

Zuzek, P.J., Nairn, R.B., Thieme, S.J., 2003. Spatial and temporal considerations for calculating shoreline change rates in the Great Lakes basin. Spatial Mapping and Change Analysis. In: Byrnes, M.R., Crowell, M., and Fowler, C. (Eds), J. Coast. Res., Special Edition 38, 125–146.

TABLE CAPTIONS

Table 1: Summary of nine inputs initially considered, and the eight adopted, in the BN model: 2007-2015 retreat rate is the BN response variable. Basic statistics and data-bin (class) boundaries are shown. Groundwater flux was not used in the selected eight-input BN. The 2007-2015 retreat rate is the BN response variable; MSL is mean sea level datum; LL is Spring 2015 average lake level.

Table 2: Single-input BN model success at predicting bluff-crest retreat rate (in order of decreasing success).

Table 3: Summary of k-fold cross validation model-selection results. For 511 BNs with combinations of 1 to 9 inputs, the model with the largest percentage of correct classifications within each BN group is listed. Among all BNs compared, the model with eight inputs (Row 8; bold italics) had the largest percentage of correct classifications and was selected as the optimal BN.

Table 4: Summary of sensitivity analysis of the eight-input BN showing the effects of removing a single input on the mean predicted posterior probability (84.1%) of the BN (in order of decreasing importance).

Table 5: Updated BNs illustrating changes in bluff attributes and processes, relative to the prior BN, associated with Low-WIH and High-WIH constraints.

Table 6: Updated BNs comparing bluff-attribute states for Low-WIH and High-WIH constraints.

Table 7: Updated BNs comparing bluff-attribute states for Lowest-LTRR (stable) and Highest-LTRR constraints.

FIGURE CAPTIONS

Figure 1: Locations of seven 1-2 km field sites (1STGL through 7BMDR) within the WECLC littoral cell that extends from the OH-PA state line to the Presque Isle flying sand spit. Six HUC-12 watersheds are shown. Scale bar (lower left) is ~3 km in length. (base maps: modified from pawalter.psu.edu and nyseagrant.org)

Figure 2: Northward looking cross-section along the WECLC showing bluff-crest elevations (from 2015 lidar), major creeks and minor ravines, generalized stratigraphy, lakefront extent of HUC-12 watersheds, Spring 2015 lake level, and BN-study sites (1STGL - 7BMDR).

Figure 3: Variability in selected environmental variables: 2007 beach width, bluff slope, and beach thickness at WECLC sites. These attributes were expected to influence bluff retreat in a BN model. Easting coordinates are in UTM meters.

Figure 4: Average annual crest change rates (m/yr) at WECLC sites for 1938-2015, 1938-2007 (training window), and 2007-2015 (validation window). Positive rates (apparent progradation) are discounted to zero (no change; see text), negative rates indicate retreat, and Easting coordinates are in UTM meters.

Figure 5: BN model for bluff retreat on the WECLC coast showing model variables and their observed distributions. See Table 1 for data details. Discretization ranges (bins) and observed probability densities (bars) are shown. Boxed ranges on the LTRR input indicate stability/unresolvable change (<0.1 m/yr), low retreat rates (0.1 – 0.3 m/yr), and moderate retreat rates (0.3 – 1.0 m/yr). Boxed ranges on the STRR indicate stability/unresolvable change (<0.1 m/yr), low retreat rates (0.1 – 0.2 m/yr), and moderate retreat rates (0.3 – 1.2 m/yr).

Figure 6: Observed bins (bars) and predicted bins (dots) for 2007-2015 average-annual retreat rate by DSAS transect at WECLC Sites 1STGL through 7BMDR. See Fig. 1 and Fig. 2 for site locations. Note variable x-axis (transect-ID spacing) scales. Negative rates denote crest retreat.

Figure 7: BNs showing updated input distributions when the BN is constrained to low-WIH (a) and high-WIH (b) conditions.

Figure 8: BNs showing updated input distributions when the BN is constrained to lowest-LTRR (a) and highest-LTRR conditions.

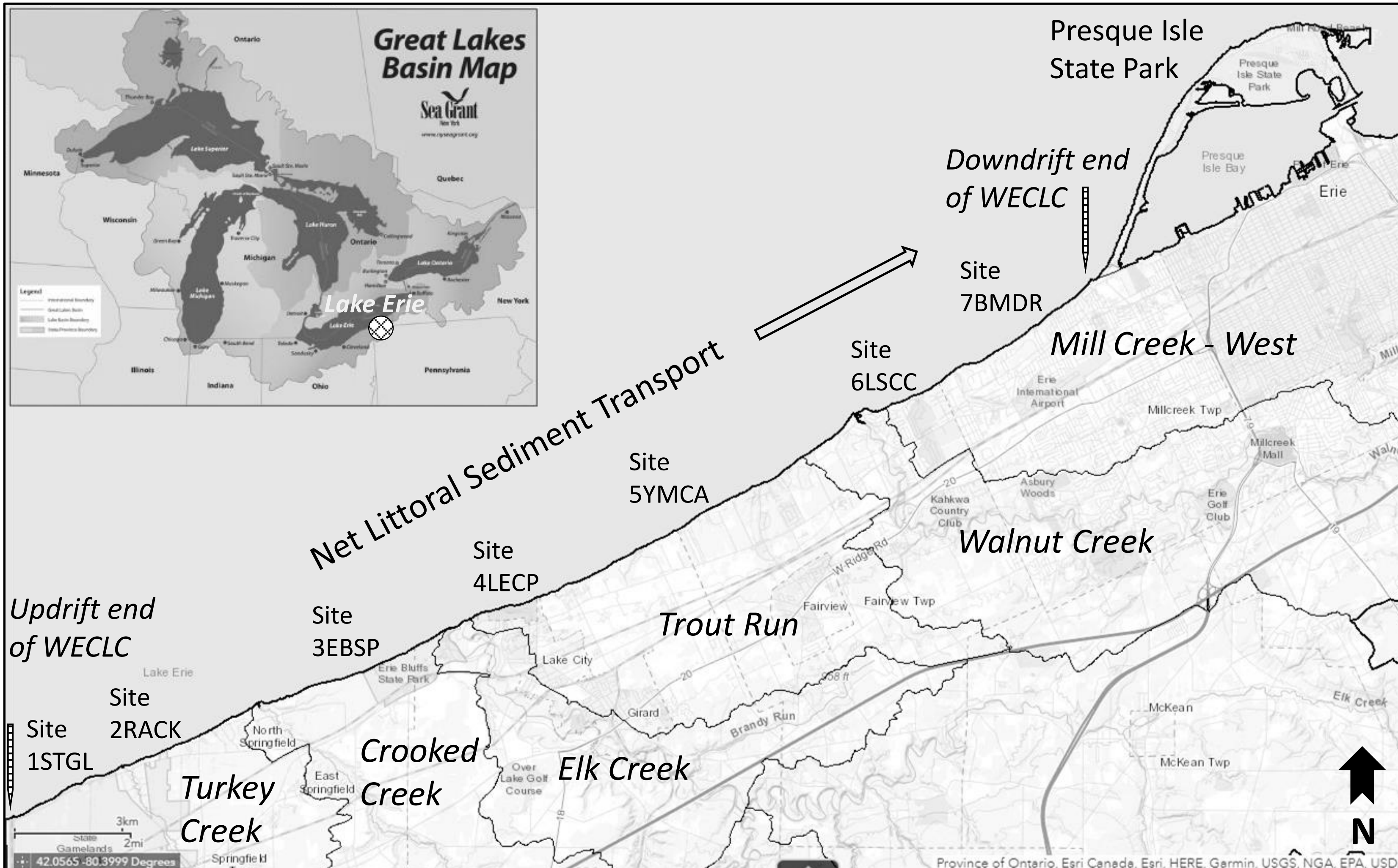

Great Lakes Basin Map
Sea Grant
Lake Erie
Presque Isle State Park
Downdrift end of WECLC
Site 7BMDR
Site 6LSCC
Mill Creek - West
Net Littoral Sediment Transport
Site 5YMCA
Site 4LECP
Site 3EBSP
Updrift end of WECLC
Site 2RACK
Site 1STGL
Walnut Creek
Trout Run
Turkey Creek
Crooked Creek
Elk Creek
N
3km
2mi
42.0565 -80.3999 Degrees
Province of Ontario, Esri Canada, Esri, HERE, Garmin, USGS, NGA, EPA, USDA

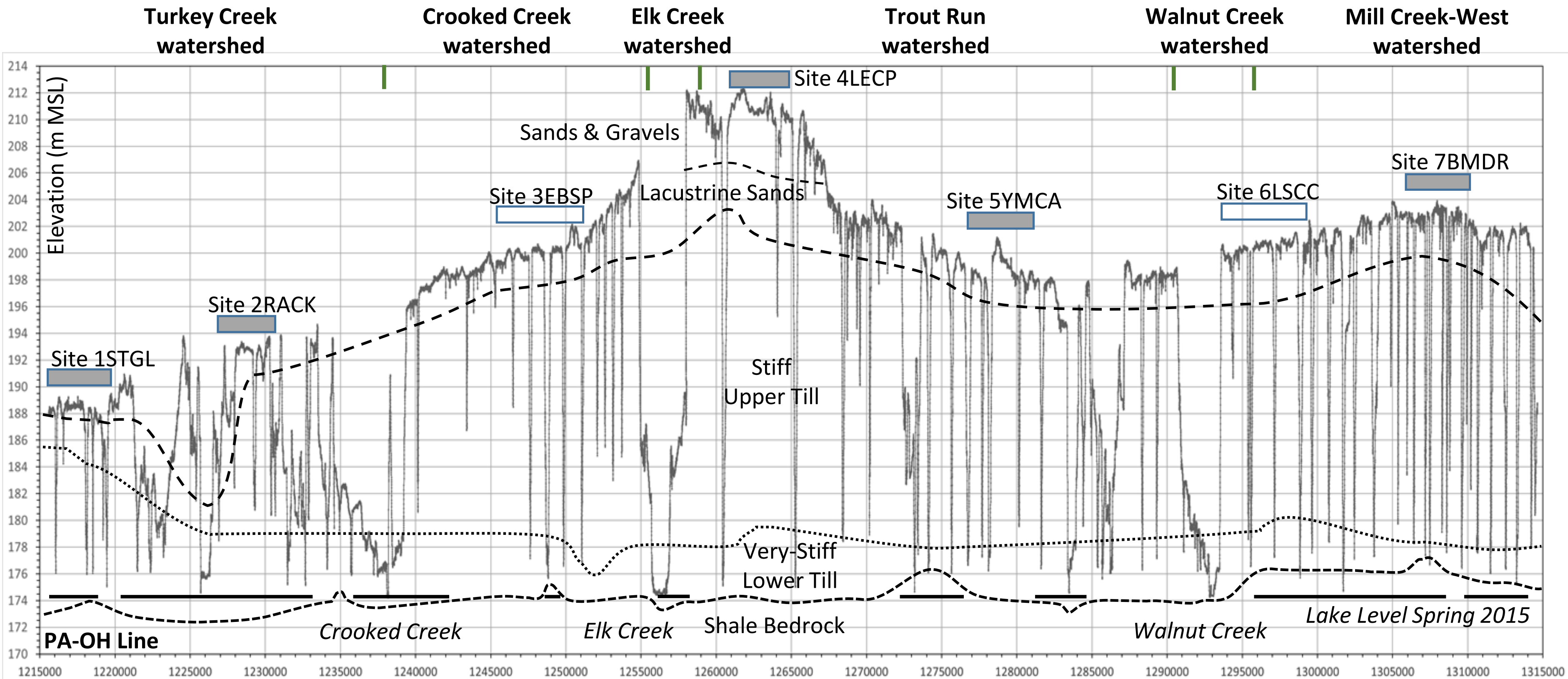

PA State Plane (ft); view to north; coast orientation N66E; 2015 lake level = 174.25 m MSL; bars = site extents

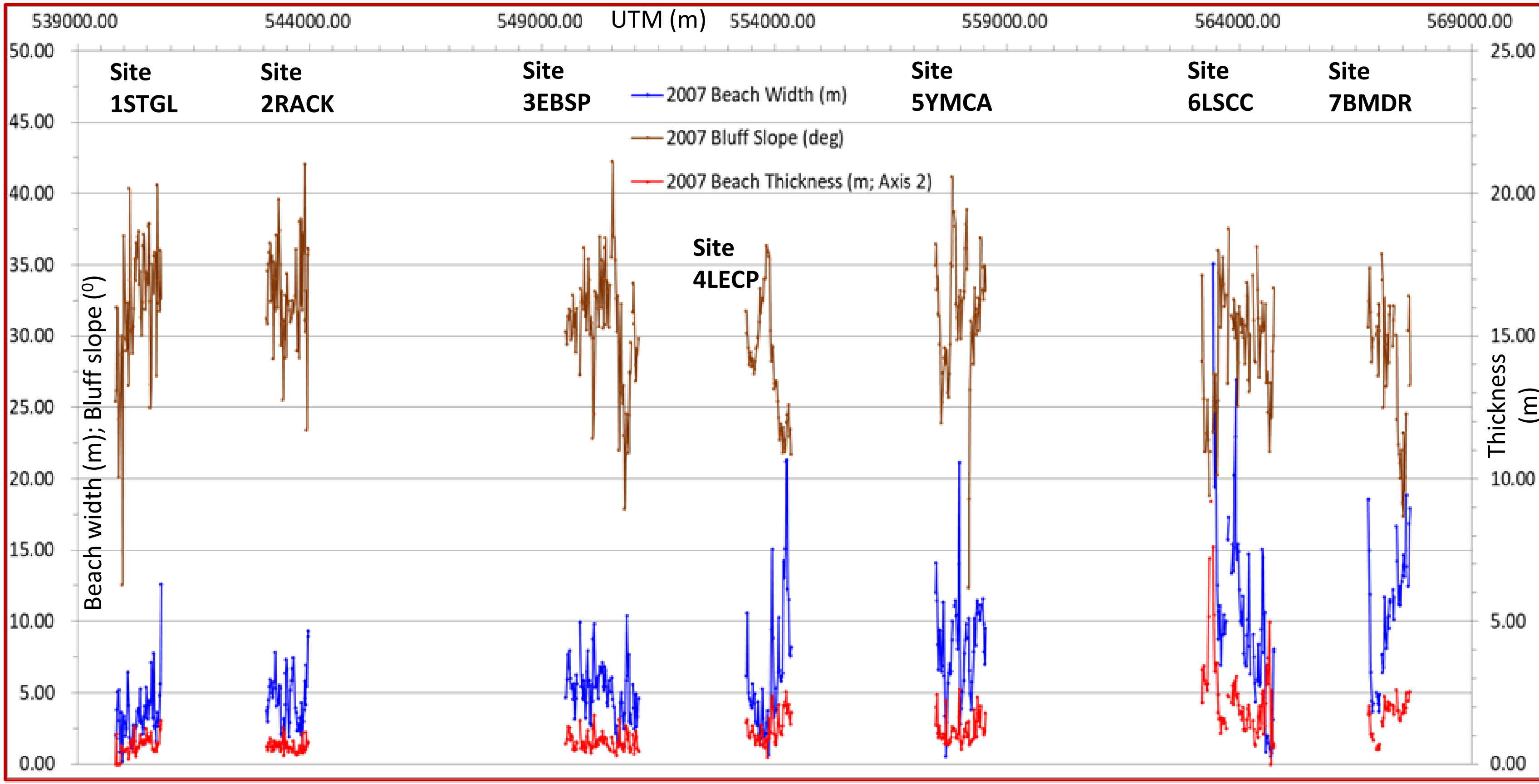
539000.00
544000.00
549000.00
UTM (m)
554000.00
559000.00
564000.00
569000.00
50.00
45.00
40.00
35.00
30.00
25.00
20.00
15.00
10.00
5.00
0.00
25.00
20.00
15.00
10.00
5.00
0.00
Site 1STGL
Site 2RACK
Site 3EBSP
Site 4LECP
Site 5YMCA
Site 6LSCC
Site 7BMDR
2007 Beach Width (m)
2007 Bluff Slope (deg)
2007 Beach Thickness (m; Axis 2)
Beach width (m); Bluff slope (°)
Thickness (m)

Foyle & Rutter: JGLR Fig. 3Gray

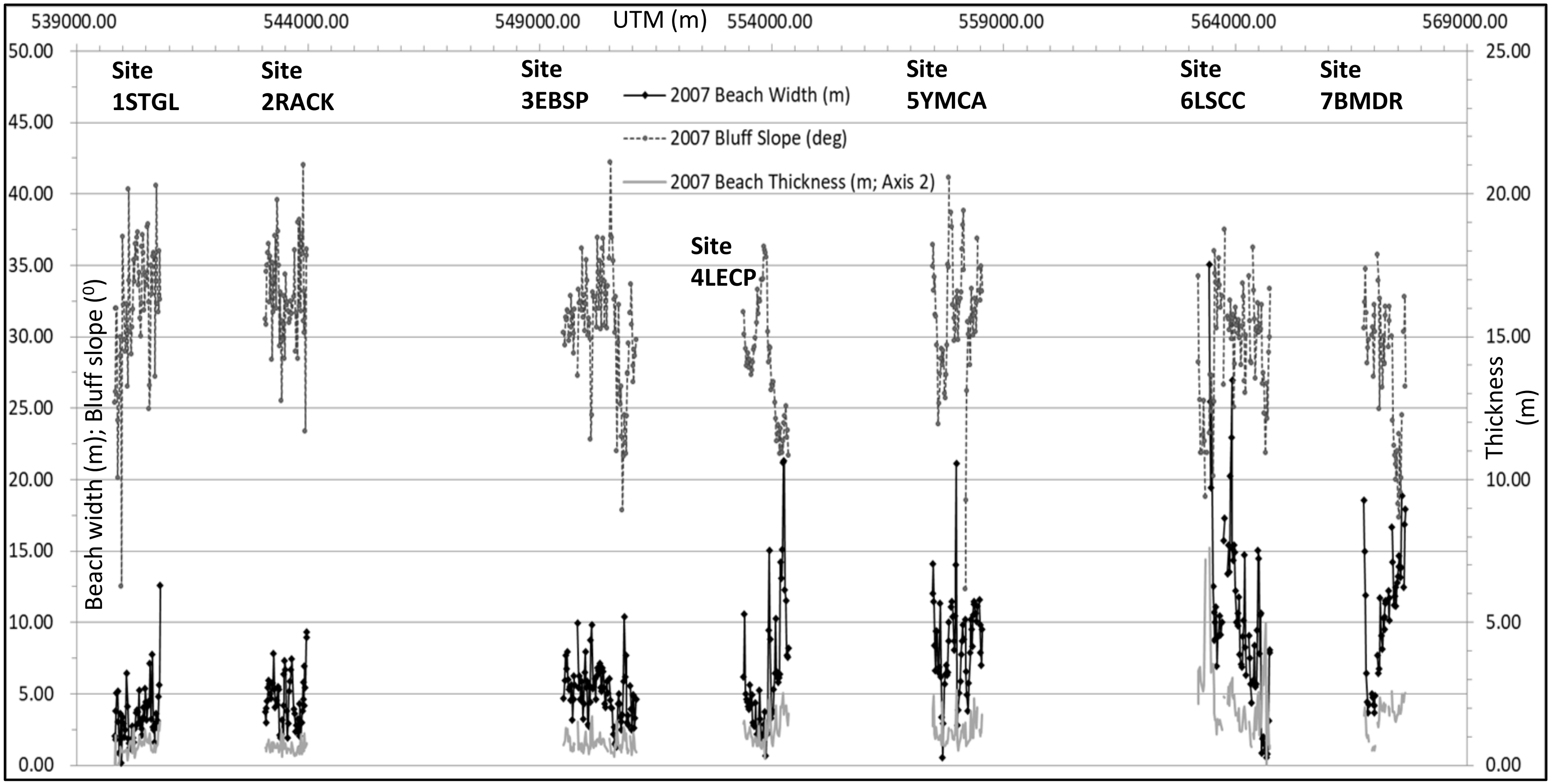

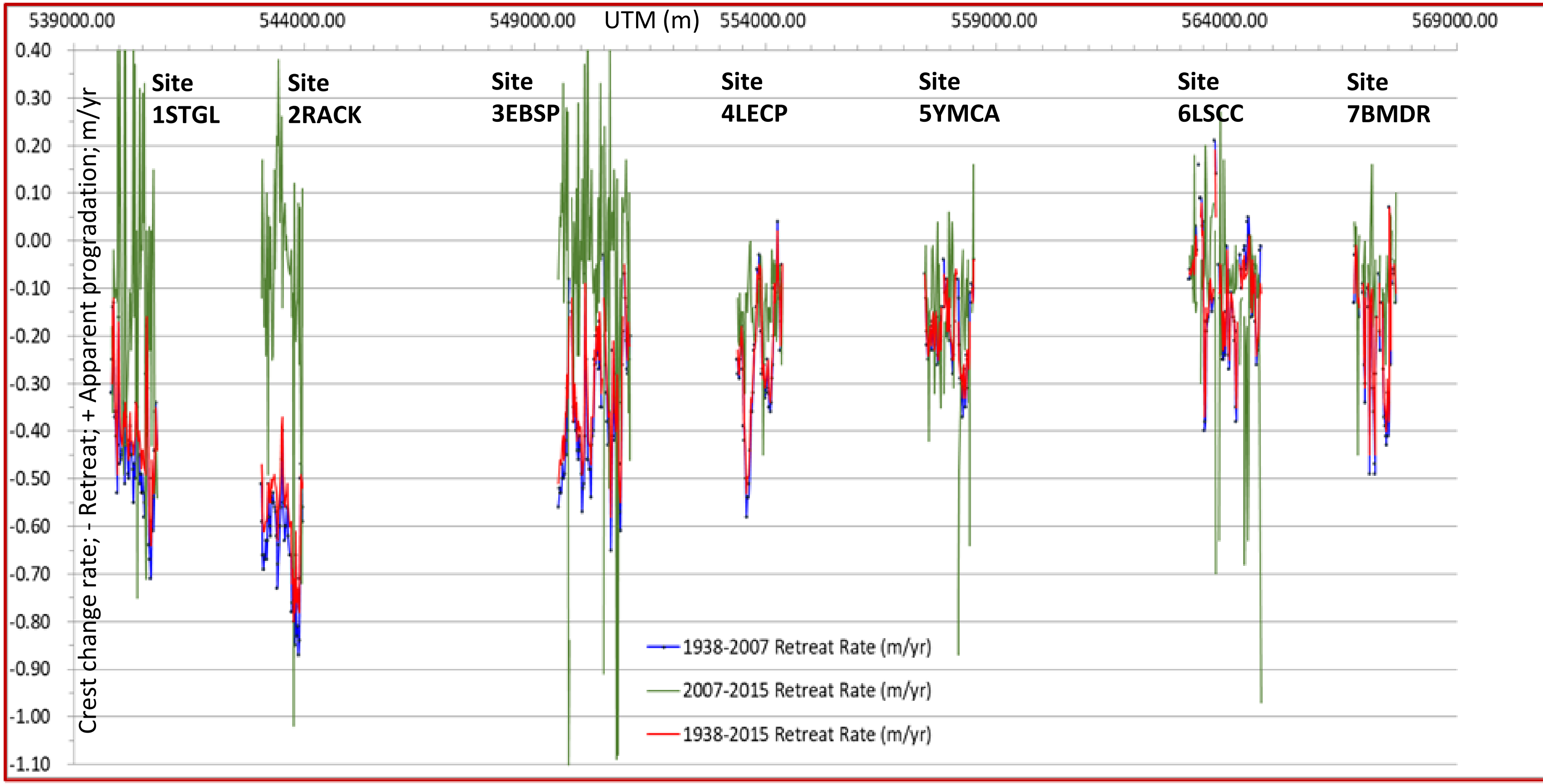

539000.00
544000.00
549000.00
UTM (m)
554000.00
559000.00
564000.00
569000.00
0.40
0.30
0.20
0.10
0.00
-0.10
-0.20
-0.30
-0.40
-0.50
-0.60
-0.70
-0.80
-0.90
-1.00
-1.10
Crest change rate; - Retreat; + Apparent progradation; m/yr
Site 1STGL
Site 2RACK
Site 3EBSP
Site 4LECP
Site 5YMCA
Site 6LSCC
Site 7BMDR
1938-2007 Retreat Rate (m/yr)
2007-2015 Retreat Rate (m/yr)
1938-2015 Retreat Rate (m/yr)

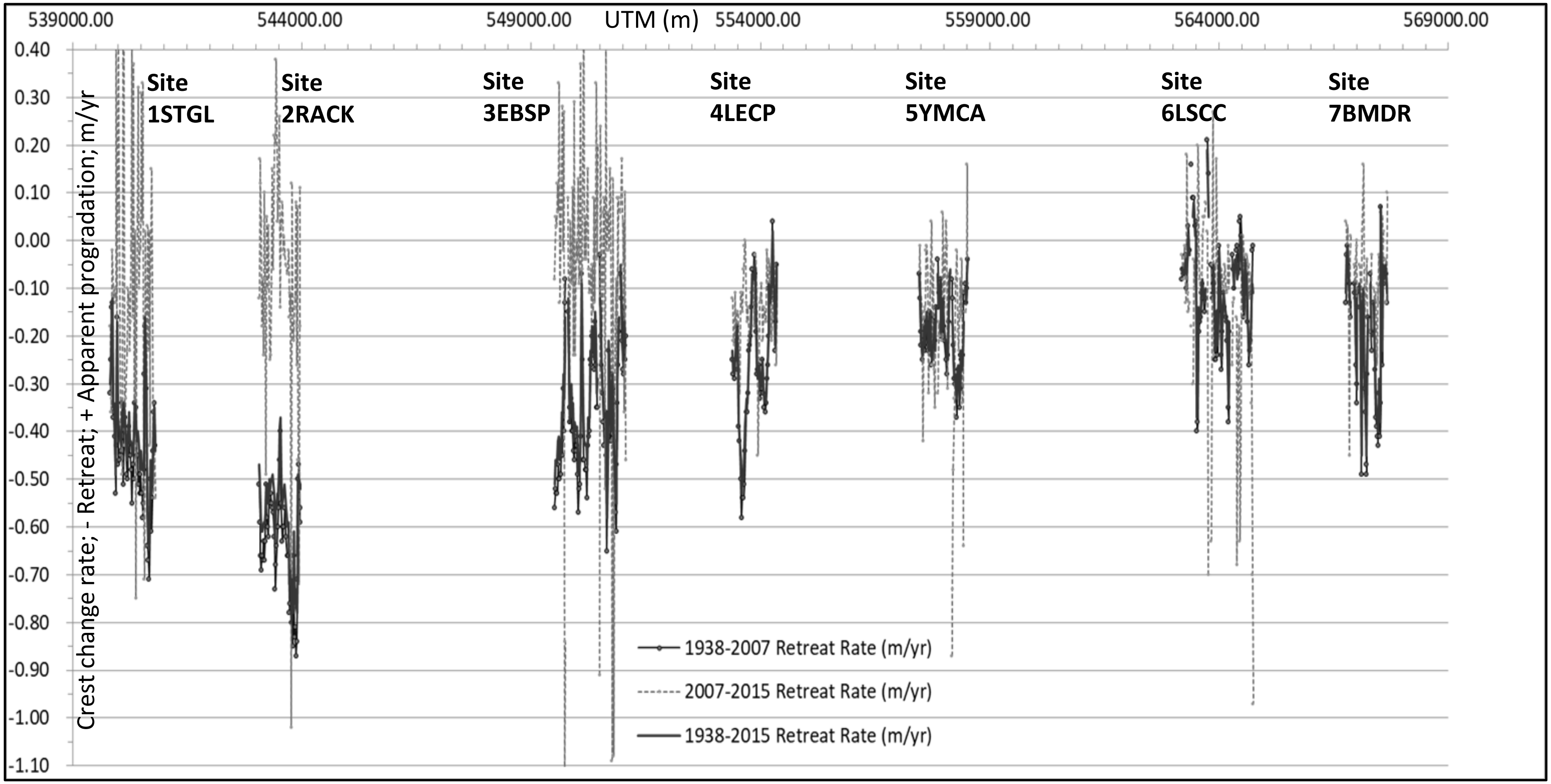

539000.00
544000.00
549000.00
UTM (m)
554000.00
559000.00
564000.00
569000.00
0.40
0.30
0.20
0.10
0.00
-0.10
-0.20
-0.30
-0.40
-0.50
-0.60
-0.70
-0.80
-0.90
-1.00
-1.10
Crest change rate; - Retreat; + Apparent progradation; m/yr
Site 1STGL
Site 2RACK
Site 3EBSP
Site 4LECP
Site 5YMCA
Site 6LSCC
Site 7BMDR
1938-2007 Retreat Rate (m/yr)
2007-2015 Retreat Rate (m/yr)
1938-2015 Retreat Rate (m/yr)

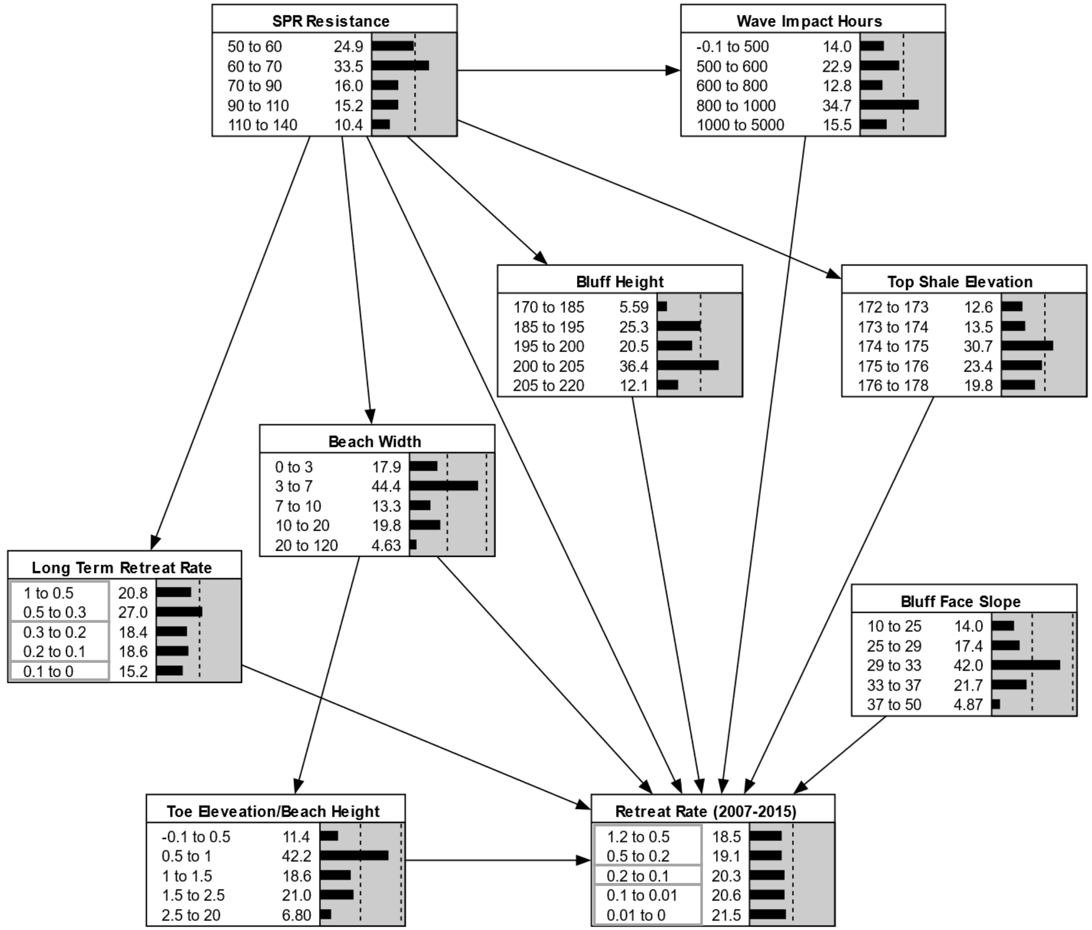
SPR Resistance
50 to 60 24.9
60 to 70 33.5
70 to 90 16.0
90 to 110 15.2
110 to 140 10.4
Wave Impact Hours
-0.1 to 500 14.0
500 to 600 22.9
600 to 800 12.8
800 to 1000 34.7
1000 to 5000 15.5
Bluff Height
170 to 185 5.59
185 to 195 25.3
195 to 200 20.5
200 to 205 36.4
205 to 220 12.1
Top Shale Elevation
172 to 173 12.6
173 to 174 13.5
174 to 175 30.7
175 to 176 23.4
176 to 178 19.8
Beach Width
0 to 3 17.9
3 to 7 44.4
7 to 10 13.3
10 to 20 19.8
20 to 120 4.63
Long Term Retreat Rate
1 to 0.5 20.8
0.5 to 0.3 27.0
0.3 to 0.2 18.4
0.2 to 0.1 18.6
0.1 to 0 15.2
Bluff Face Slope
10 to 25 14.0
25 to 29 17.4
29 to 33 42.0
33 to 37 21.7
37 to 50 4.87
Toe Eleveation/Beach Height
-0.1 to 0.5 11.4
0.5 to 1 42.2
1 to 1.5 18.6
1.5 to 2.5 21.0
2.5 to 20 6.80
Retreat Rate (2007-2015)
1.2 to 0.5 18.5
0.5 to 0.2 19.1
0.2 to 0.1 20.3
0.1 to 0.01 20.6
0.01 to 0 21.5

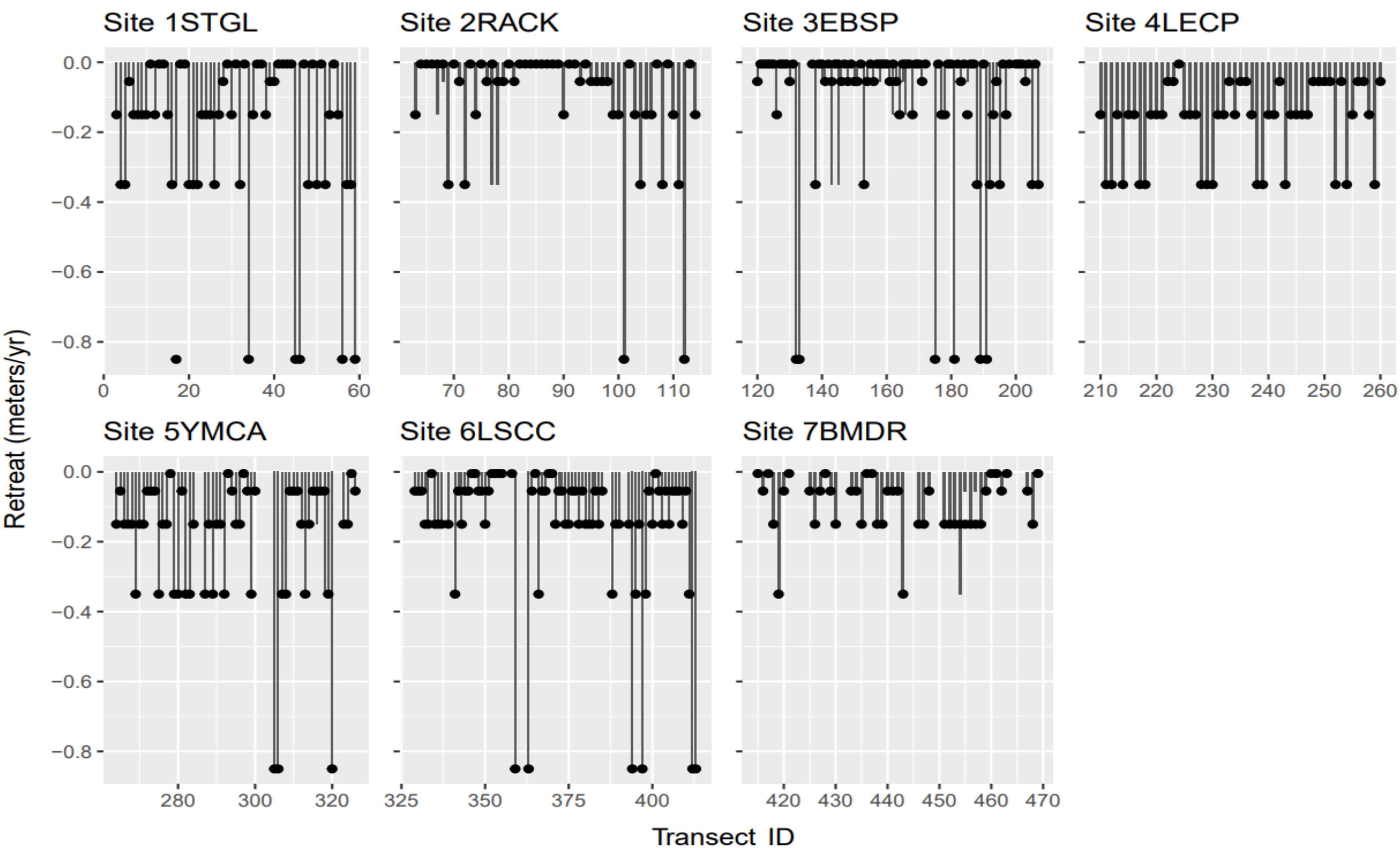
Site 1STGL
Site 2RACK
Site 3EBSP
Site 4LECP
Site 5YMCA
Site 6LSCC
Site 7BMDR
Retreat (meters/yr)
0.0
−0.2
−0.4
−0.6
−0.8
0
20
40
60
70
80
90
100
110
120
140
160
180
200
210
220
230
240
250
260
280
300
320
325
350
375
400
420
430
440
450
460
470
Transect ID

Foyle & Rutter: JGLR 2022 Fig. 7 a, b

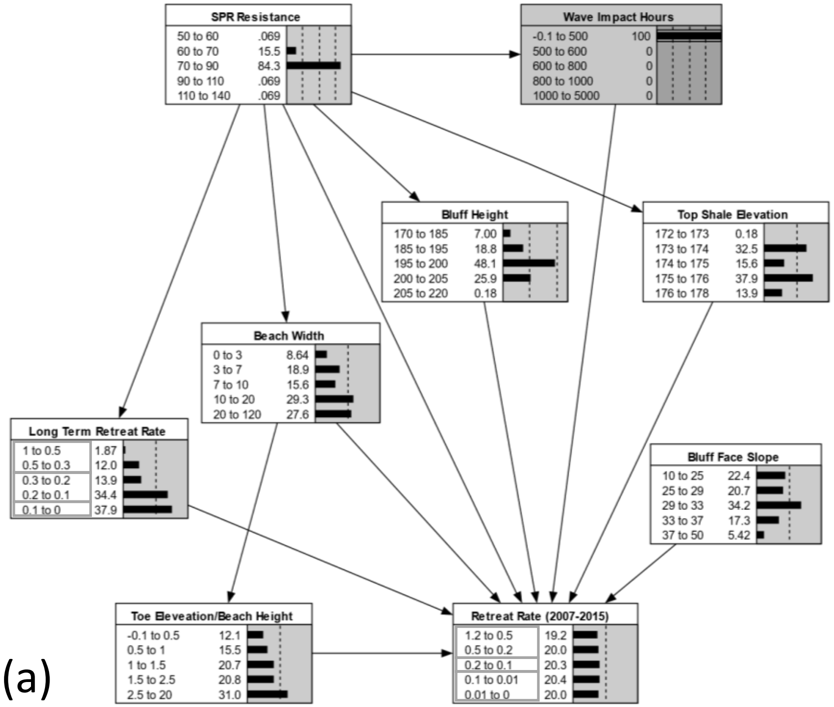

(a)

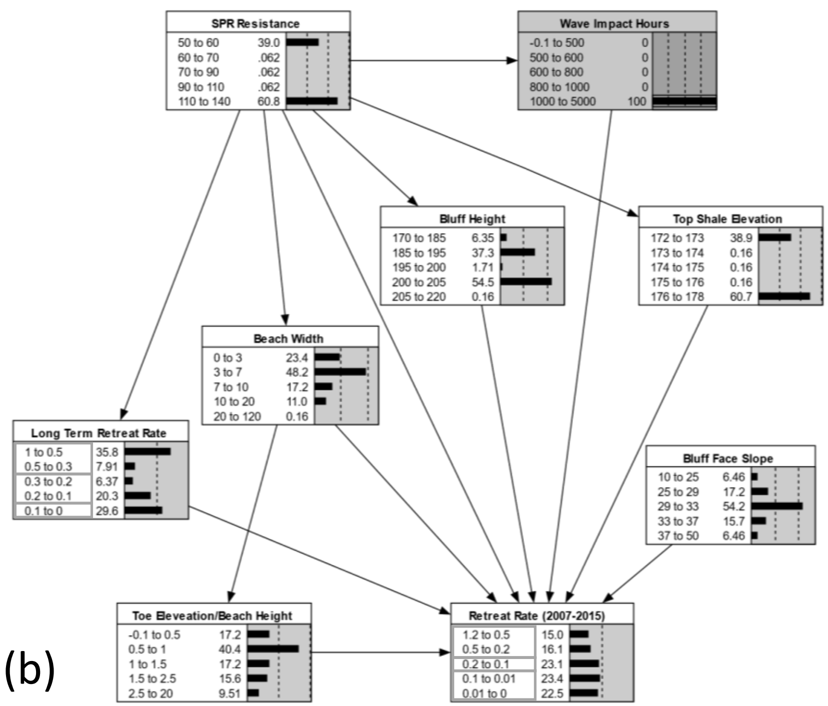

(b)

Foyle & Rutter: JGLR Fig. 8 a, b

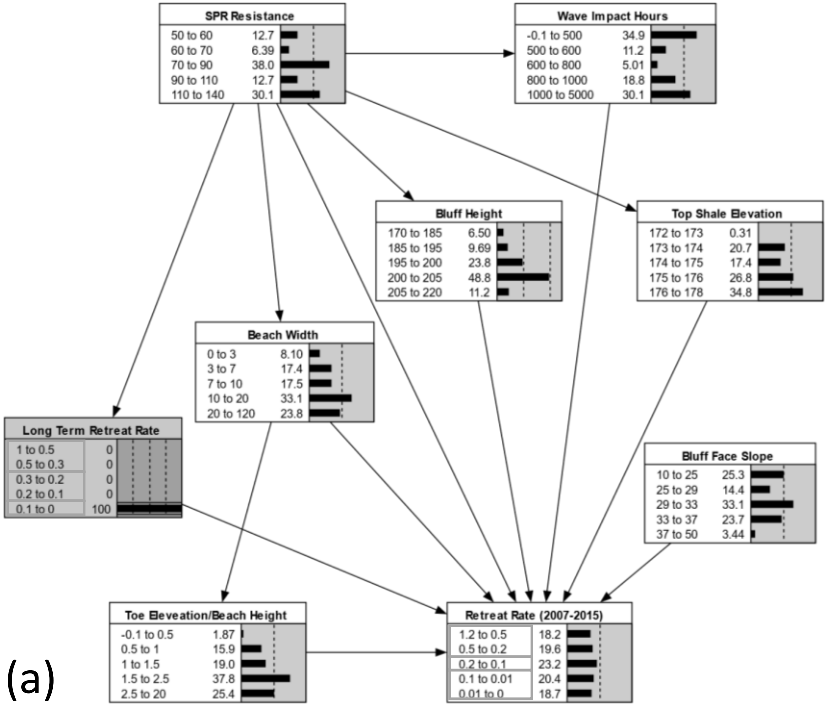

(a)

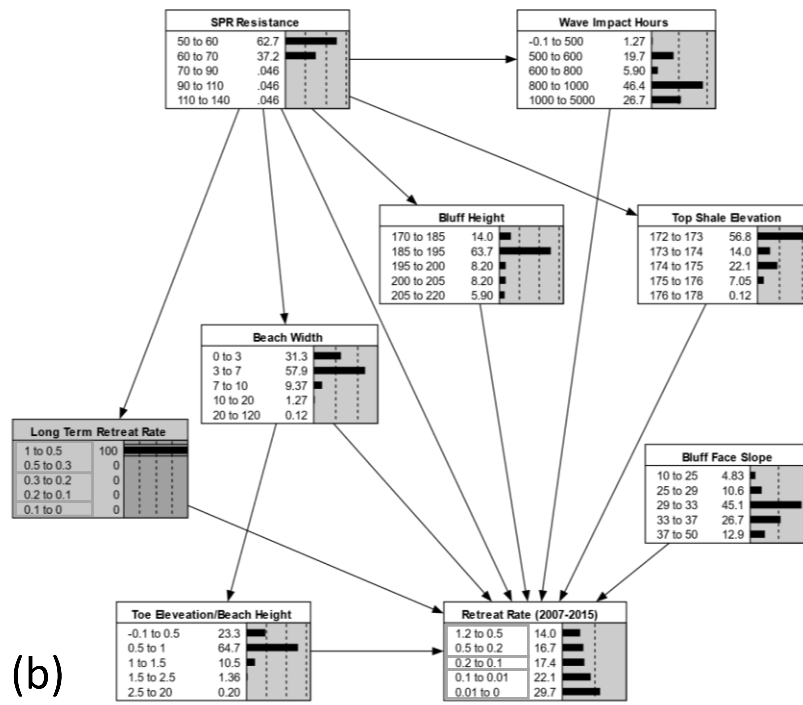

(b)

Table 1: Summary of nine inputs initially considered, and the eight adopted, in the BN model: 2007-2015 retreat rate is the BN response variable. Basic statistics and data-bin (class) boundaries are shown. Groundwater flux was not used in the selected eight-input BN. The 2007-2015 retreat rate is the BN response variable; MSL is mean sea level datum; LL is Spring 2015 average lake level.

Model Parameter	***Min***	***Mean***	***Median***	***Max***	***Boundaries for 5 Bins***
SPR Erosion Resistance (blows/m)	51	76	66	133	50-60-70-90-110-140
Wave Impact Hours (hrs/yr)	0.0	873.9	848.1	4896.1	0.1-500-600-800-1000-5000
1938-2007 Retreat Rate (m/yr)	0	0.31	0.28	0.87	0-0.1-0.2-0.3-0.5-1.0
Beach Width (m)	0.2	8.9	5.8	117.3	0-3-7-10-20-120
Bluff Crest Height (m MSL)	174.8	197.8	200.0	212.2	170-185-195-200-205-220
Top Shale Bedrock Elevation (m MSL)	172.5	174.8	174.8	177.2	172-173-174-175-176-178
Toe Elevation/Beach Height (m LL)	0.0	1.2	0.9	9.2	0-0.5-1.0-1.5-2.5-20
Groundwater Flux (m^3/ m^2/yr)	*0.1*	*36.9*	*15.0*	*222.0*	*0-5-10-20-50-250*
Bluff Face Slope (degrees)	12.3	30.3	31.0	42.2	10-25-29-33-37-50
2007-2015 Retreat Rate (m/yr)	0	0.11	0.09	1.12	0.0-0.01-0.1-0.2-0.5-1.2

Table 2: Single-input BN model success at predicting bluff-crest retreat rate (in order of decreasing success).

BN Single-Input Model	*% Correct Prediction of STRR*
Bluff Face Slope (BFS; degrees)	42%
Groundwater Flux ($m^3/m^2/yr$)	39%
SPR Erosion Resistance (SPR; blows/m)	37%
Toe Elevation/Beach Height (TE/BH; m LL)	37%
Beach Width (BW; m)	34%
Bluff Crest Height (BCH; m MSL)	34%
Wave Impact Hours (WIH; hours/yr)	34%
Long-Term Retreat Rate (LTRR; m/yr)	33%
Top Shale elevation (TS; m MSL)	32%

Table 3: Summary of k-fold cross validation model-selection results. For 511 BNs with combinations of 1 to 9 inputs, the model with the largest percentage of correct classifications within each BN group is listed. Among all BNs compared, the model with eight inputs (Row 8; bold italics) had the largest percentage of correct classifications and was selected as the optimal BN.

# of Inputs	***Correct Percent***	***Model Inputs***
1	36.8	Toe Elevation/Beach Height
2	36.3	SPR Erosion Resistance, Bluff Face Slope
3	37.2	Toe Elevation/Beach Height, Bluff Crest Height, Wave Impact Hours
4	39	Beach Prism Width, Toe Elevation/Beach Height, Top-Shale Elevation, Bluff Crest Height
5	39.5	Long-Term Retreat Rate, Bluff Face Slope, Beach Width, Toe Elevation/Beach Height, Wave Impact Hours
6	38.7	SPR Resistance, GW Flux, Long-Term Retreat Rate, Toe Elevation/Beach Height, Top-Shale Elevation, Bluff Crest Height
7	39.2	SPR Resistance, GW Flux, Bluff Face Slope, Beach Width, Toe Elevation/Beach Height, Bluff Crest Height, Wave Impact Hours
8	***39.6***	***SPR Resistance, Long-Term Retreat Rate, Bluff Face Slope, Beach Width, Toe Elevation/Beach Height, Top-Shale Elevation, Bluff Crest Height, Wave Impact Hours***
9	36.8	SPR Resistance, Long-Term Retreat Rate, Bluff Face Slope, Beach Width, Toe Elevation/ Beach Height, Top-Shale Elevation, Bluff Crest Height, Wave Impact Hours, Groundwater Flux

Table 4: Summary of sensitivity analysis of the eight-input BN showing the effects of removing a single input on the mean predicted posterior probability (84.1%) of the BN (in order of decreasing importance).

Model Input Variable	***Reduction in Prediction Probability***
Long-Term Retreat Rate (LTRR)	14.3%
Bluff Face Slope (BFS)	13.8%
Toe Elevation/Beach Height (TE/BH)	9.7%
Beach Width (m)	9.1%
Top-Shale Elevation (TS)	5.3%
Wave Impact Hours (WIH)	4.6%
Bluff Crest Height (BCH)	4.0%
SPR Erosion Resistance (SPR)	0.3%

Table 5: Updated BNs illustrating changes in bluff attributes and processes, relative to the prior BN, associated with Low-WIH and High-WIH constraints.

Input	Prior (Fig. 5)	Low-WIH (Fig. 7a)	High-WIH (Fig. 7b)
SPR (blows/m)	42% >70 BPM	84% >70 BPM; unimodal	61% >70 BPM ; bimodal
LTRR (m/yr)	Moderate rates dominant	Low rates dominant	Moderate rates dominant
- Highest >0.5 (m/yr)	21%	2%	36%
- Low & stable <0.3 (m/yr)	52%	86%	56%
- Stable <0.1 (m/yr)	15%	38%	30%
BW (m)	62% <7 m wide	28% <7 m wide	72% <7 m wide
BCH (m MSL)	49% >200 m median	26% >200 m median	55% >200 m median
TS >176m (m MSL)	20%	14%	61%
TE/BH >1.5 (m LL)	28%	52%	25%
BFS >29 (degrees)	69%	57%	76%
STRR (m/yr)	Skews slightly low	Skews slightly higher	Skews slightly lower

Table 6: Updated BNs comparing bluff-attribute states for Low-WIH and High-WIH constraints.

Input	**Low-WIH Conditions at Bluff (Fig. 7a)**		**High-WIH Conditions at Bluff (Fig. 7b)**	
SPR (blows/m)	More resistant	84% >70 BPM	Less resistant	61% >70 BPM
LTRR (m/yr)	Slower	14% >0.3 m/yr	Faster	44% >0.3 m/yr
BW (m)	Wider	28% <7 m	Narrower	72% <7 m
BCH (m; MSL)	Unimodal distribution	26% >200 m	Bimodal distribution	55% >200 m
TS (m MSL)	Low-dominant	14% >176 m	High-dominant	61% >176 m
TE/BH (m LL)	High-dominant	52% >1.5 m	Low-dominant	25% >1.5 m
BFS (degrees)	Gentler	57% $>29^0$	Steeper	76% $>29^0$
STRR (m/yr)	Slightly higher rates	39% >0.2 m/yr	Slightly lower rates	31% >0.2 m/yr

Table 7: Updated BNs comparing bluff-attribute states for Lowest-LTRR (stable) and Highest-LTRR constraints.

Input	**Lowest-LTRR (Stable) Conditions (Fig. 8a)**		**Highest-LTRR Conditions (Fig. 8b)**	
SPR (blows/m)	More resistant	81% >70 BPM	Less resistant	0% >70 BPM
WIH (hrs/yr)	Less intense run-up	51% <800 hrs/yr	More intense run-up	27% <800 hrs/yr
BW (m)	Wider	26% <7 m	Narrower	89% <7 m
BCH (m MSL)	Taller	60% >200 m	Lower	14% >200 m
TS (m MSL)	High-dominant	35% >176 m	Low-dominant	0.1% >176 m
TE/BH (m LL)	Thick beach/tall toe	63% >1.5 m	Thin beach/low toe	2% >1.5 m
BFS (degrees)	Gentler	60% >29^{0}	Steeper	85% >29^{0}
STRR (m/yr)	Slightly higher rates	38% >0.2 m/yr	Slightly lower rates	31% >0.2 m/yr